Measurements of Lateral Spread Using a Real Time Kinematic Global Positioning System

April 2002

Report by:

Loren L. Turner, P.E.
California Department of Transportation
Division of New Technology & Research
5900 Folsom Blvd. MS-5
Sacramento CA 95819
(916) 227-7174
loren.turner@dot.ca.gov

Project No. F-2001-OR-05 65-680422
Continuous GPS: Pilot Applications
Phase II

Geotechnology Implementation
Caltrans
Office of Infrastructure Research

Table of Contents

1.0 Introduction

This report presents deformation measurements collected during two full-scale lateral spread tests in Japan using a networked Real-Time Kinematic Global Positioning System (RTK-GPS).

With recent advancements in GPS technologies, measurements of ground surface displacements under static as well as dynamic conditions have become easier to obtain with increased accuracy and reduced costs (Langley 1998). Late in 1999, the California Department of Transportation (Caltrans) initiated a focused research effort to look into innovative GPS technologies and applications (Turner 2000, 2001). The primary objective of the research was to evaluate the feasibility of applying GPS in the study of geotechnical phenomenon through the development, integration, and test deployment of a GPS-based instrumentation package utilizing emerging high precision RTK-GPS and wireless communications technologies. The instrumentation package was configured primarily for the remote monitoring of landslide movements. However, a unique opportunity arose to test deploy the system in a full scale earthquake experiment at a shipping port facility in northern Japan in November and December 2001.

2.0 Full-Scale Lateral Spread Tests in Japan

2.1 Background

A unique opportunity arose to deploy the Networked RTK system in a controlled test environment for two full-scale earthquake tests conducted in Japan in late 2001. The intention of study was to collect data on the response of civil structures such as bridge foundations, sea walls, and utility pipelines during severe loading induced by earthquakes (Ashford 2001). When shaken, loose saturated sandy soils can undergo a dramatic loss of strength known as *liquefaction*. The occurrence of liquefaction can lead to large ground deformations, or *lateral spread*, that may impart forces on these structures that, to date, are not well understood or quantifiable. Forces due to lateral spread are illustrated in Figure 1. Two full-scale seismic tests were conducted by using controlled blasting techniques to induce liquefaction and lateral spread.

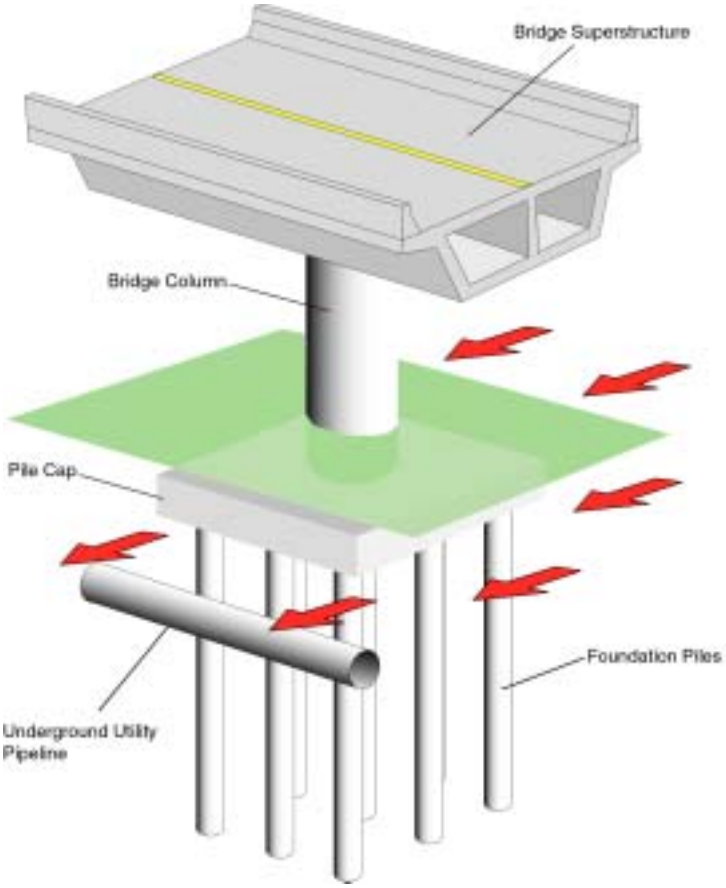

Figure 1 – Lateral spread imparts forces on bridge foundations and lifelines.

A team of researchers from Caltrans were invited to assist with two full-scale seismic tests conducted at the Port of Tokachi on the island of Hokkaido, Japan. The team was led by Loren Turner and included Cliff Roblee and Tom Shantz from the Division of New Technology and Research.

The results presented here were part of an internationally-partnered project involving several universities, research institutes, industrial participants, and governmental agencies from Japan and the United States. The U.S. sponsors

supporting the investigation of lateral spread effects on lifeline components are from the Lifelines Program of the Pacific Earthquake Engineering Research (PEER) Center that includes the California Department of Transportation, the California Energy Commission, and the Pacific Gas & Electric Company. The Japanese sponsors include the Japan Port and Airport Research Institute (PARI), the Japan Civil Engineering Research Institute, Waseda University, University of Tokyo, Kyoto University, Sato Kogyo, Kanden Kogyo, Tokyo Electric Power Company, Japan Gas Association, Japan Association for Marine Structures, Japan Association for Steel Piles, and the Japan Reclamation and Dredging Association.

Accurate measurements of ground deformations during the generated seismic events were a critical component of the research and are extremely difficult to obtain by conventional instrumentation techniques. The use of the GPS network in the Japan tests provided the opportunity to strengthen the experimental control on liquefaction while further demonstrating the Networked RTK systems' capabilities for future remote monitoring applications envisioned for Caltrans.

2.2 Description of the Test Site

The two tests were conducted at the Port of Tokachi, a commercial shipping facility primarily used to transport concrete products and raw materials. As part of a relatively recent effort to expand the port operations and its capacity,

additional work areas were created through the conventional use of sea walls and fills. This practice involved the installation of perimeter quay walls which were subsequently filled by hydraulically placing soils. The soil type, the construction method, and groundwater conditions all contributed to a site highly susceptible to liquefaction and lateral spread.

For the first test in November 2001, the test site was comprised of an area approximately 25m wide by 100m long. One end of the site was bordered by a large waterway with the soil retained by a quay wall as shown in Figure 2. Moving away from the water, the ground surface sloped gently upwards such that the other end of the site was approximately 2.00m higher. The ground surface elevation near the sea wall was +3.00m, and the ground surface elevation at the top of the slope was +5.00m. The waterway elevation fluctuated throughout the day, as did the groundwater elevation, between 0.00m and +1.50m as a result of the proximity to the Pacific Ocean. The entire test area was surrounded by sheet piling installed to tip elevation –5.00m Figure 3 shows the site layout.

Figure 2 – November 2001 test site.

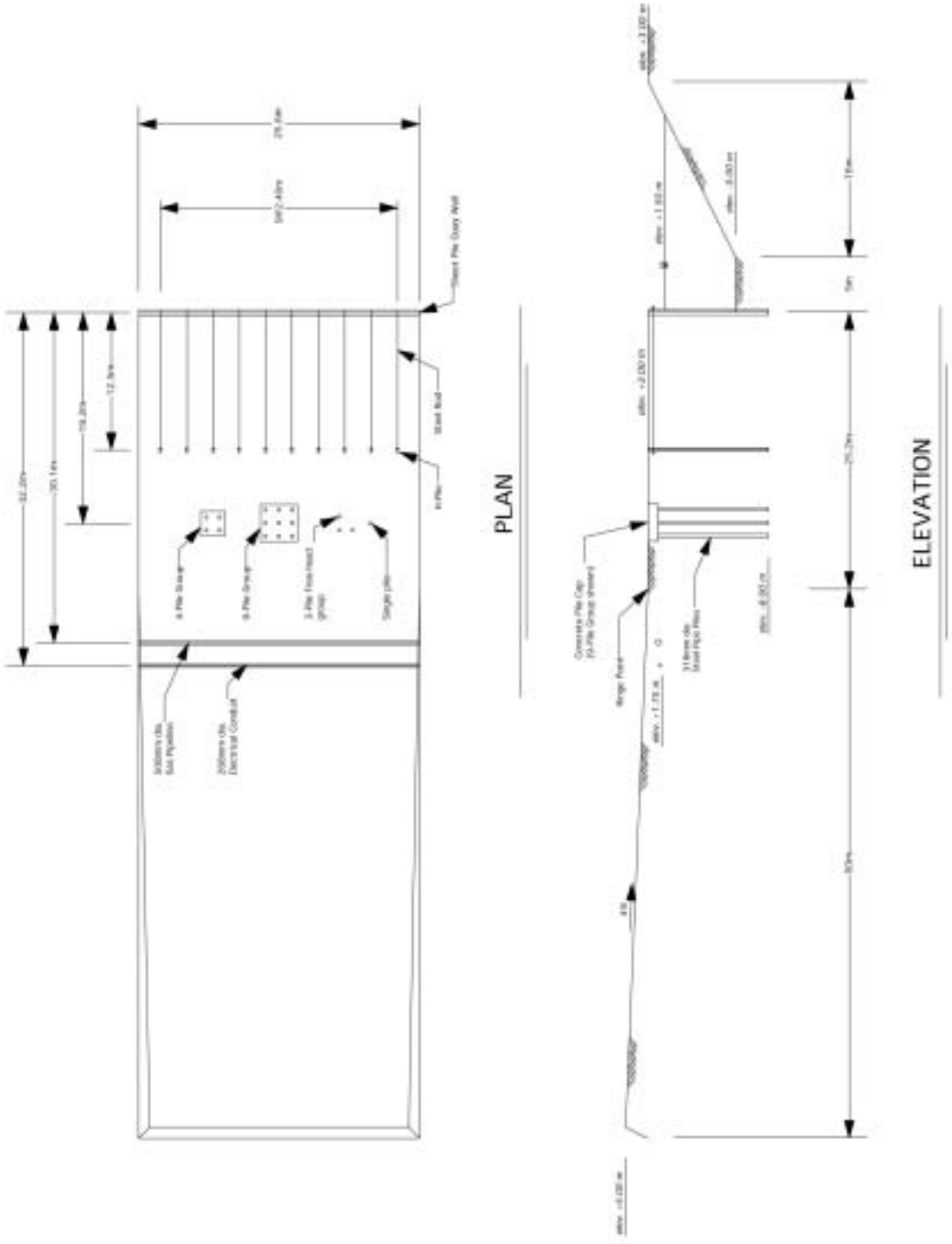

Figure 3 – Test Site Layout, November 2001 Test

For the second test in December 2001, the test site was significantly modified in an attempt to induce additional ground deformations. The quay walls and perimeter sheet piling installed as part of the first test were removed, since they tended to impede displacements. Additionally, the test site was regraded to create a steeper slope as shown in Figures 4 and 5.

Figure 4 – December 2001 test site.

Several full-scale test specimens were placed within the test zone for evaluation under lateral spread. These included four sets of pipe pile foundations and three underground utility pipelines. Figures 3 and 5 show the locations of the test specimens.

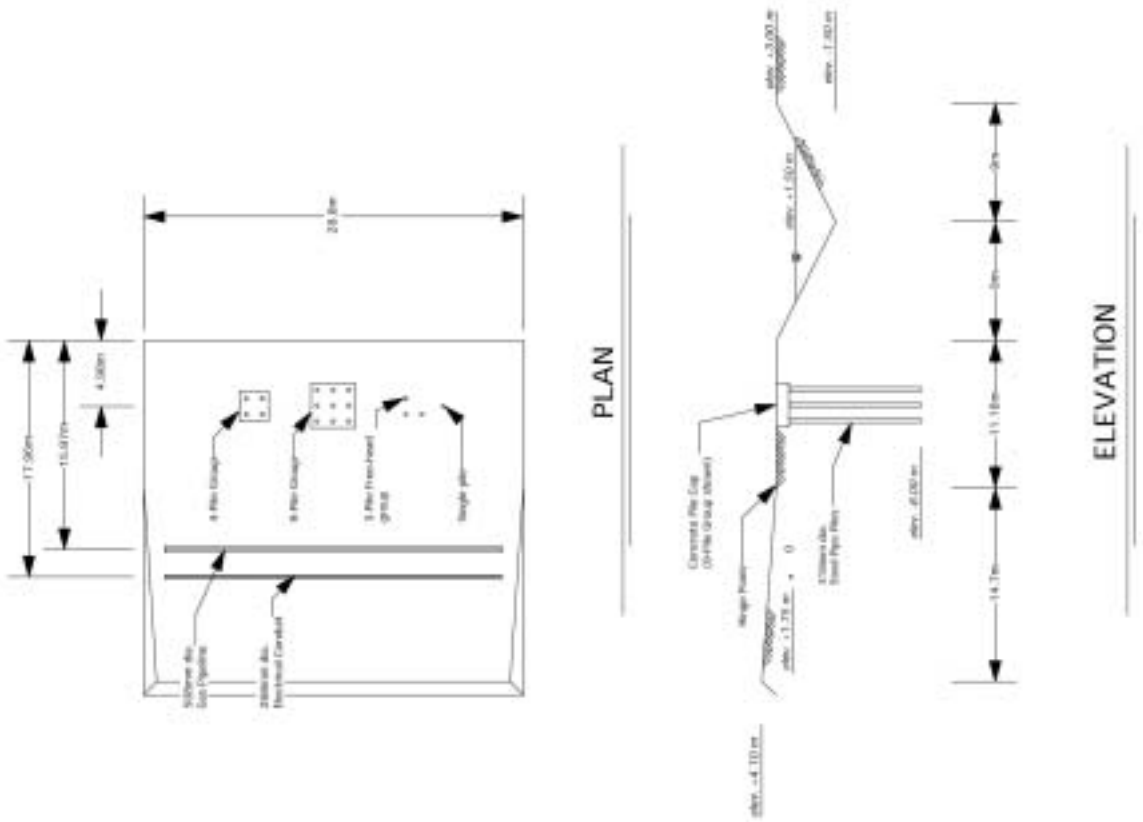

Figure 5 – Test Site Layout, December 2001 Test

Subsurface conditions at the site were characterized by hydraulically placed sandy fill underlain by very dense native gravels. Very loose sand extended from a ground surface elevation of +3.00m down to elevation –0.40m. Uncorrected standard Penetration Test blow counts ranged from 1 to 5 blows per foot in this layer. From elevation –0.40m to elevation –4.30m was very loose sandy and clayey silt. Uncorrected standard Penetration Test blow counts ranged from 0 to 2 blows per foot in this layer. Below elevation –4.30m the soil was found to be medium dense sand to very dense gravel with uncorrected standard Penetration Test blow counts greater than 50 blows per foot.

The pipe piles for all of the deep foundations were 318mm diameter with wall thickness of 10.5mm, a nominal length of 10m, and constructed of 400MPa yield strength steel. Piles were installed using impact driving methods. In two of the deep foundations, the pile tops were fixed from rotation by reinforced concrete pile caps that were 1m thick. This included a nine pile group arranged in a 3x3 matrix, and a four pile group arranged in a 2x2 matrix, both employing 3.5 pile diameters center-to-center spacing for the piles. Most of the piles in these two groups were driven full length to an approximate elevation of –8.00m. These piles were driven well into the denser soils to generate fixity at the pile tips. A three pile group was installed at 3.5 pile diameters center-to-center spacing without a pile cap allowing free rotation at the pile head. On average, these piles

were driven to an approximate elevation of –5.60m leaving 1.40m of the pile above ground. Since these piles were not driven far into the denser soil layer, fixity of the pile tips was not certain. Finally, a single pile was installed, also allowing for free rotation at the pile head. This pile was driven to elevation –9.67m leaving 0.33m of the pile above ground. As with the four pile and nine pile groups, this pile was driven well into the denser soils to generate fixity at the pile tip.

Although three underground utility pipelines were installed and instrumented in the test site, only two of them were instrumented with GPS sensors. The two pipelines, a gas pipeline and an electrical conduit, were oriented transversely across the site and were anchored at either end to the sheet pile wall bordering the site limits. The connections to the sheet pile wall were designed to allow for some rotation at the ends of the pipes. The gas pipeline consisted of a 508mm diameter pipe with a wall thickness of 6mm and yield strength of 400MPa. The electrical conduit consisted of a 268mm diameter pipe with a wall thickness of 6mm and yield strength of 400MPa. Both pipelines were approximately 25m in length. The two pipelines were installed within 2m of each other in a single excavated trench 3.10m wide and 1.45m deep. The bottoms of both pipelines were set at elevation +1.75m. The trench was backfilled in multiple compacted layers.

2.3 Deployment of the GPS Field Units

A total of twelve GPS units were deployed for the tests. Two of the units served as reference base stations at an offsite monitoring center. The ten remaining units were deployed throughout the site to measure movements of the ground surface, pile foundations, and pipelines. Each of the ten field units were comprised of a GPS receiver and antenna, wireless data transceiver and antenna, and battery backup power system. The equipment was packaged in small weatherproof enclosures to which the GPS and wireless transceiver antennas were attached as shown in Figure 6. The components of a typical field unit consisting of the equipment enclosure, wireless transceiver antenna, and GPS antenna are shown in Figure 7.

Figure 6 – Equipment enclosure housing the GPS receiver, wireless equipment, and backup power system

Figure 7 – Typical field unit with equipment enclosure (left), wireless transceiver antenna (center), and GPS antenna (right).

The locations of the GPS field units are summarized in Tables 1 and 2, and Figures 8 and 9, for the November and December tests, respectively. The layouts for both tests were identical with the exception of the location of Unit 2E.

GPS Unit Desig.	Location of GPS Antenna
1A	Mounted to concrete pile cap for 9-pile group
1B	Mounted directly to top of slope inclinometer casing, ~1.6m in front of 9-pile group
1C	Mounted to raft and secured to slope inclinometer casing, ~6.9m in front of 9-pile group
1D	Mounted to the top of the single pile
1E	Mounted to slope inclinometer casing, ~1.0m in front of the single pile
2A	Mounted to concrete pile cap for 4-pile group
2B	Mounted to raft and secured to slope inclinometer casing, ~10.4m in front of 4-pile group
2C	Mounted to the top of the leading pile in the 3-pile free-headed pile group.
2D	Mounted to a vertical post affixed to the gas pipeline
2E	Mounted to a vertical post affixed to the electrical conduit

Table 1 – Location of GPS field units for November 2001 test

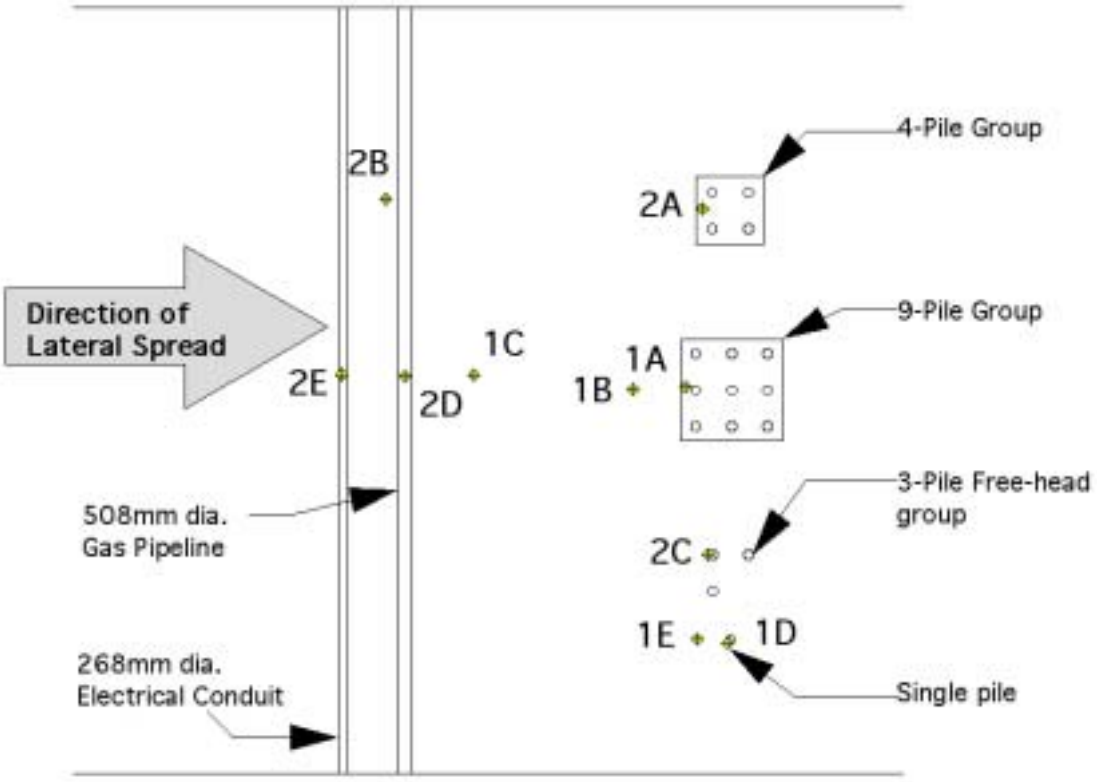

Figure 8 – Layout of GPS field units for November 2001 test

GPS Unit Desig.	Location of GPS Antenna
1A	Mounted to concrete pile cap for 9-pile group
1B	Mounted directly to top of slope inclinometer casing, ~1.5m in front of 9-pile group
1C	Mounted directly to top of slope inclinometer casing, ~7.2m in front of 9-pile group
1D	Mounted to the top of the single pile
1E	Mounted directly to top of slope inclinometer casing, ~1.0m in front of the single pile
2A	Mounted to concrete pile cap for 4-pile group
2B	Mounted directly to top of slope inclinometer casing, ~10.8m in front of 4-pile group
2C	Mounted to the top of the leading pile in the 3-pile free-headed pile group.
2D	Mounted to a vertical post affixed to the gas pipeline
2E	Mounted directly to top of slope inclinometer casing, between 4-pile and 9-pile groups

Table 2 – Location of GPS field units for December 2001 test

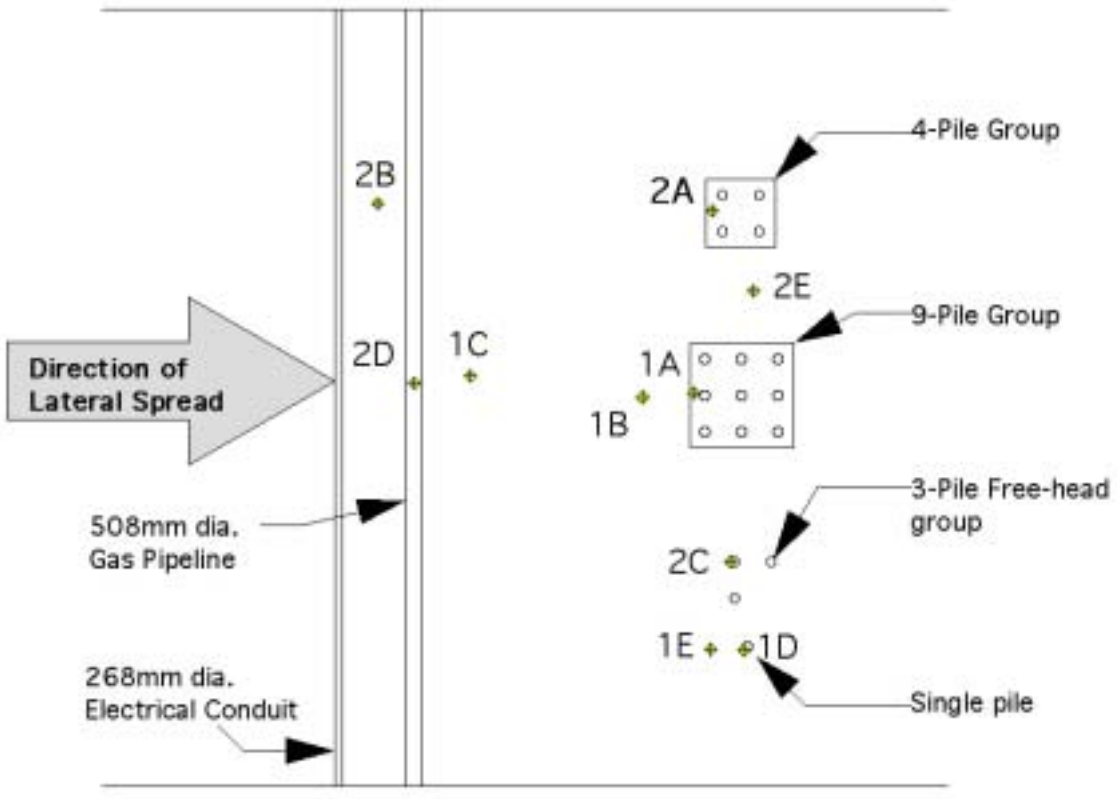

Figure 9 – Layout of GPS field units for December 2001 test

The center of the GPS antenna for Unit 1A was located near the front edge on the concrete pile cap for the 9-pile group. The mid-height of the antenna was positioned 43.5cm above the top concrete surface using steel brackets and threaded rod. The antenna was mounted at this location for both the November and December tests. Figure 10 provides details on the installation of the GPS antenna at this location.

The center of the GPS antenna for Unit 1B was located on top of a slope inclinometer casing. The antenna was mounted on to a threaded rod which was attached to the inclinometer casing. For the November test the mid-height of the antenna was positioned 51.2cm above the ground surface (approximated by the elevation of the surface of the pile cap) and 17.5cm above the top of the inclinometer casing. For the December test the mid-height of the antenna was positioned 66.6cm above the ground surface. Figure 10 shows the dimensions of the position for both the November and December tests for Unit 1B.

The GPS receiver, wireless communications, and power components for Units 1A and 1B were housed in a weatherproof enclosures which were then secured to the pile cap for the 9-pile group. Photos of the installation of Units 1A and 1B for the November test are shown in Figures 11 and 12. A photo of Unit 1A for the December test is shown in Figure 13.

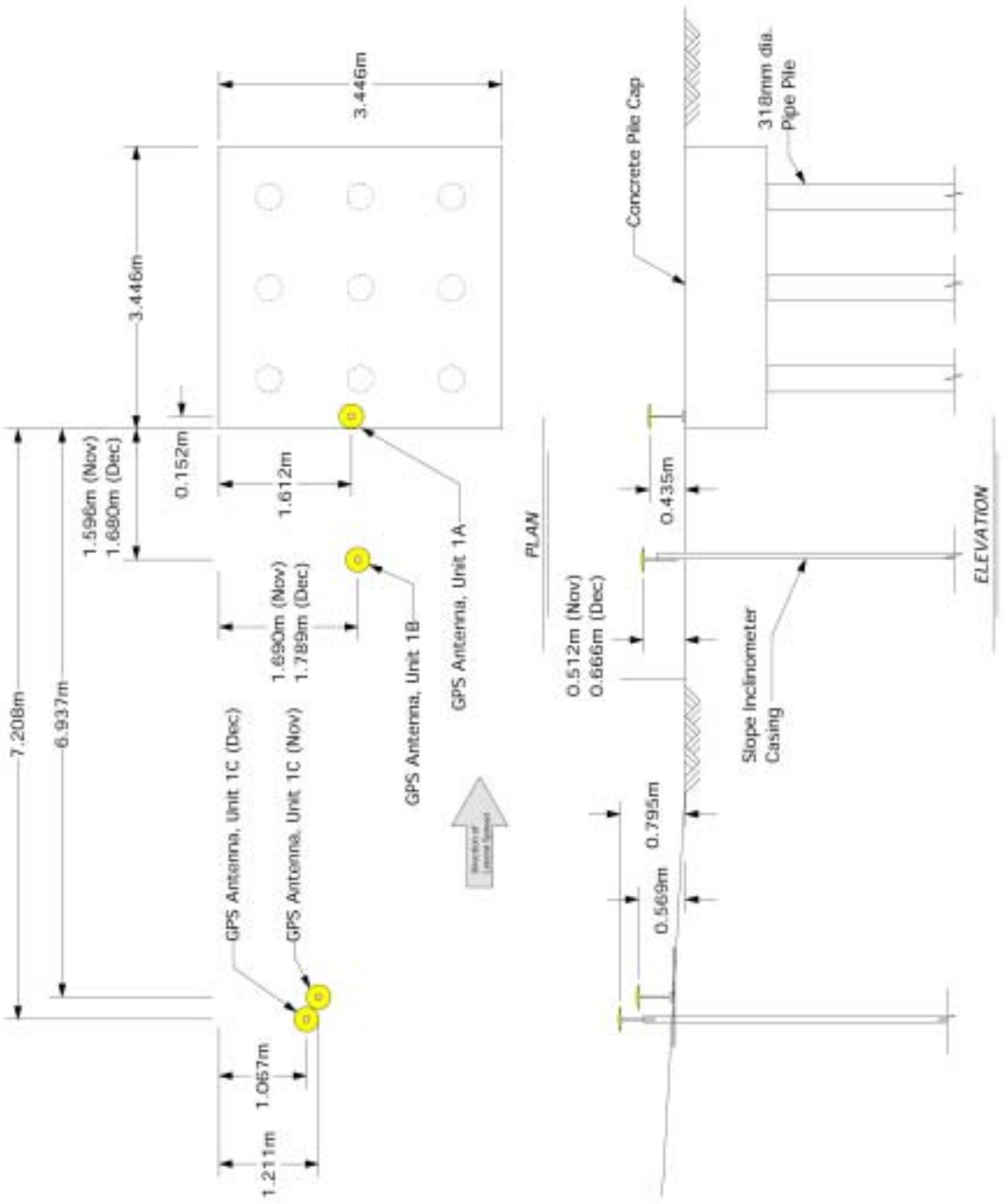

Figure 10 – Position of Units 1A, 1B, and 1C

Figure 11 – Units 1A and 1B, November Test

Figure 12 – Units 1A and 1B, November Test

Figure 13 – Unit 1A, December Test

Unit 1C was affixed to a raft that was tethered to a nearby slope inclinometer casing for the November test. The purpose of this particular installation method was to measure an average displacement of the ground at the location of the inclinometer casing while removing any secondary displacements resulting from tilting and rotation of the casing. To this end a square 1.2m by 1.2m raft was constructed from 10mm thick plywood. The mid-height of the antenna was positioned 42.5cm above the raft surface using steel brackets and threaded rod as shown in Figure 14. The raft was attached to the slope inclinometer casing using steel tie wire and was anchored to the ground using wooden stakes driven approximately 45cm into the soil. A separate raft was constructed to support the

enclosure for the GPS receiver, wireless communications, and power components.

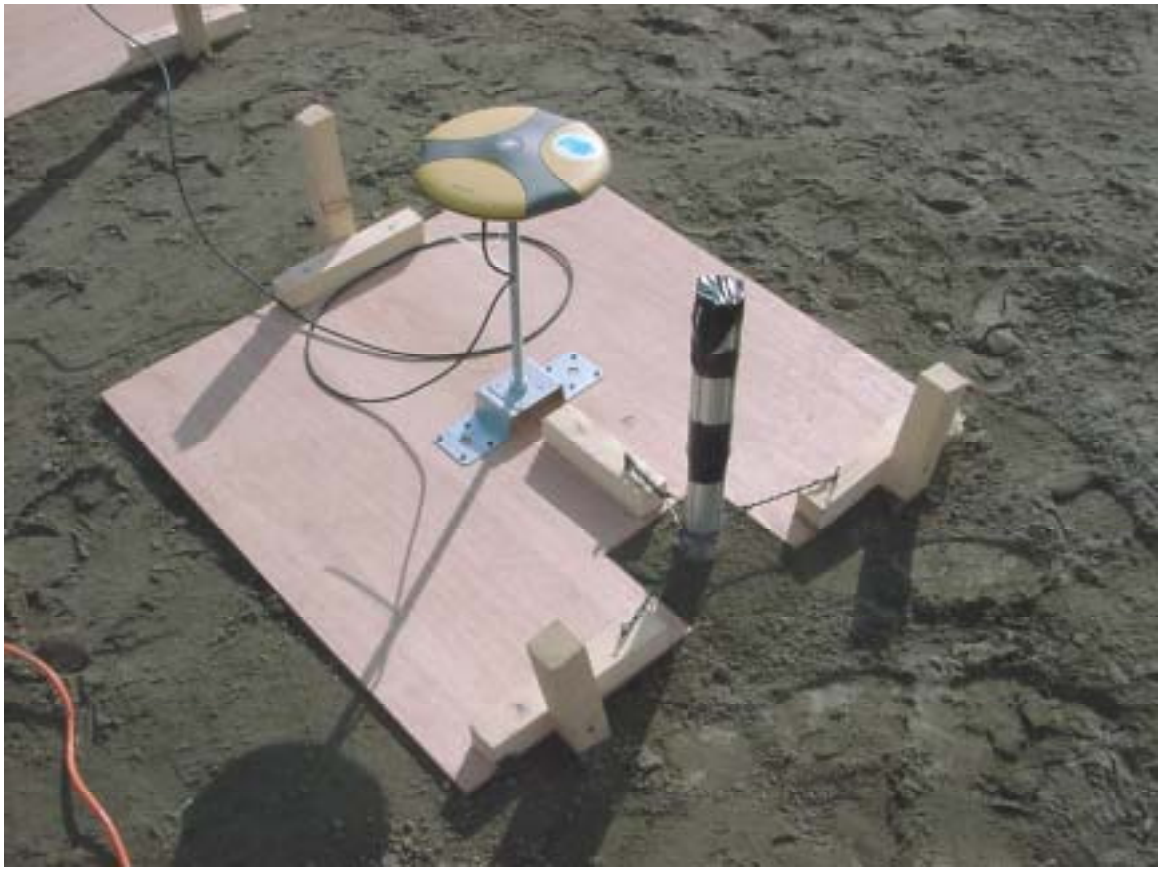

Figure 14 – Unit 1C, November test

For the December test, the raft was not used, and the GPS antenna was located on top of the slope inclinometer casing as shown in Figure 15. The antenna was mounted on to a threaded rod which was attached to the inclinometer casing. The mid-height of the antenna was positioned 79.5cm above the elevation of the surface of the pile cap. Details of both the November and December installation of Unit 1C are shown in Figure 10.

Figure 15 – Unit 1C, December test

Units 1D, 1E, and 2C were positioned to monitor the displacements of the free-head pile specimens and the surrounding ground surface as shown in Figure 16. Unit 1D was mounted to the single pile specimen. The mid-height of the GPS antenna was positioned 35.3cm above the top of the pile and approximately 77.5cm above the ground surface. Unit 1E was mounted to the top of a slope inclinometer casing and was positioned 17.5cm above the top of the pile and approximately 66.5cm above the ground surface. This unit was set approximately 1m in front of the single pile to provide a measurement of near field ground displacements for the pile during the lateral spread.

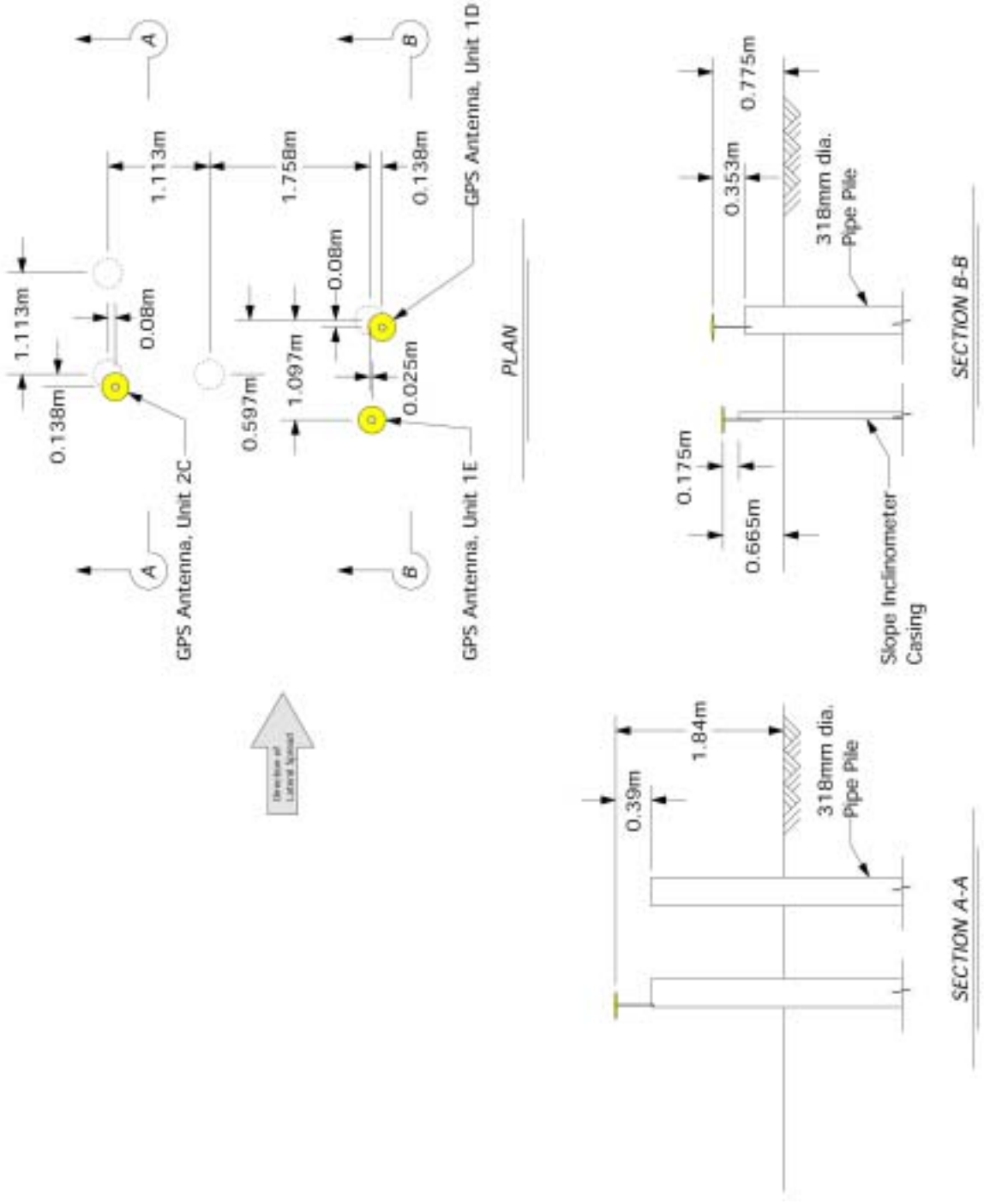

Figure 16 - Position of Units 1D, 1E, and 2C

Unit 2C was mounted to top of the leading pile in the 3-pile free head group. The mid-height of the GPS antenna was mounted 39.0cm above the pile top and approximately 184.0cm above the ground surface. For all of these units, threaded rod and steel brackets were used to secure the antennas to the piles or casings.

The GPS receiver, wireless communications, and power components for Units 1D, 1E, and 2C were housed in a weatherproof enclosures which were attached by wire to the piles. Photos of the installation of Units 1D, 1E, and 2C are shown in Figures 17 and 18.

Figure 17 – Units 1D and 1E, November test

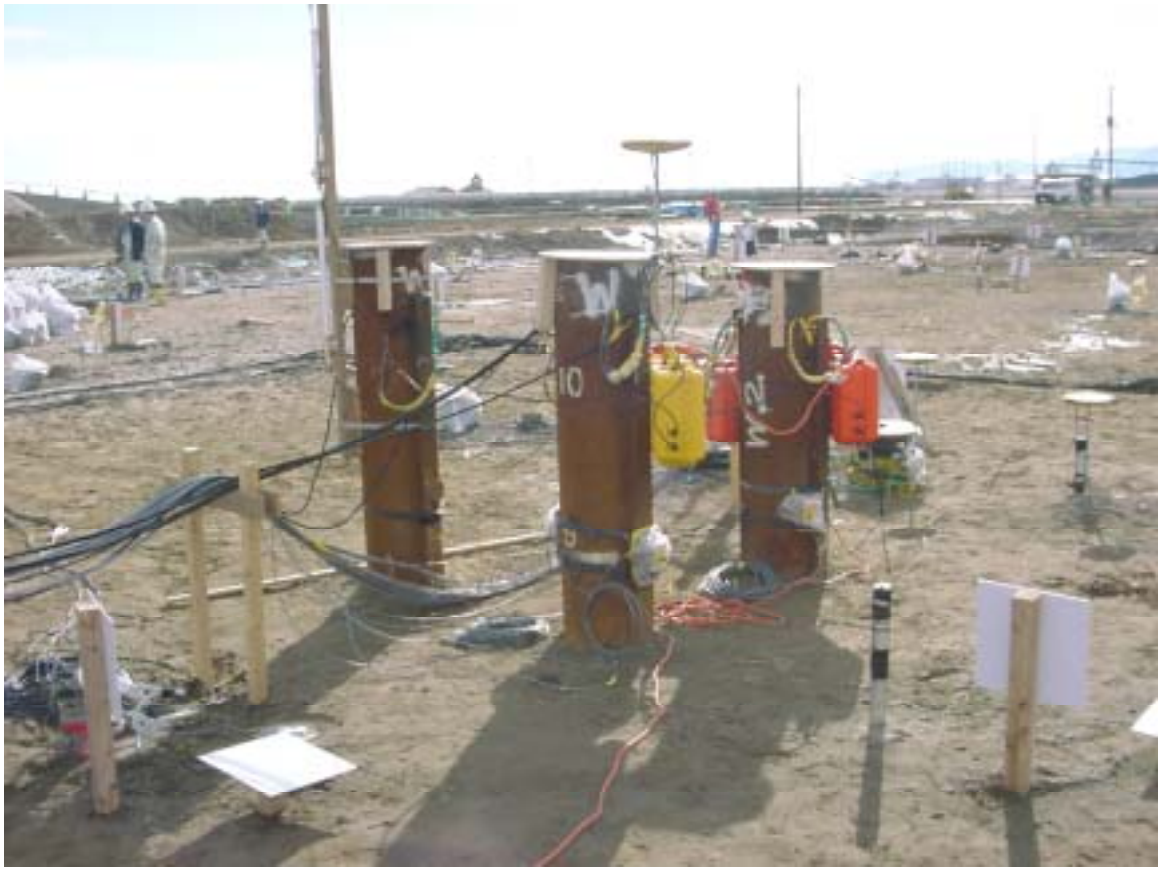

Figure 18 – Units 1D, 1E, and 2C, November test

The center of the GPS antenna for Unit 2A was located near the front edge on the concrete pile cap for the 4-pile group. The mid-height of the antenna was positioned 43.5cm above the top concrete surface using steel brackets and threaded rod. The antenna was mounted at this location for both the November

and December tests. Figure 19 provides details on the installation of the GPS antenna at this location.

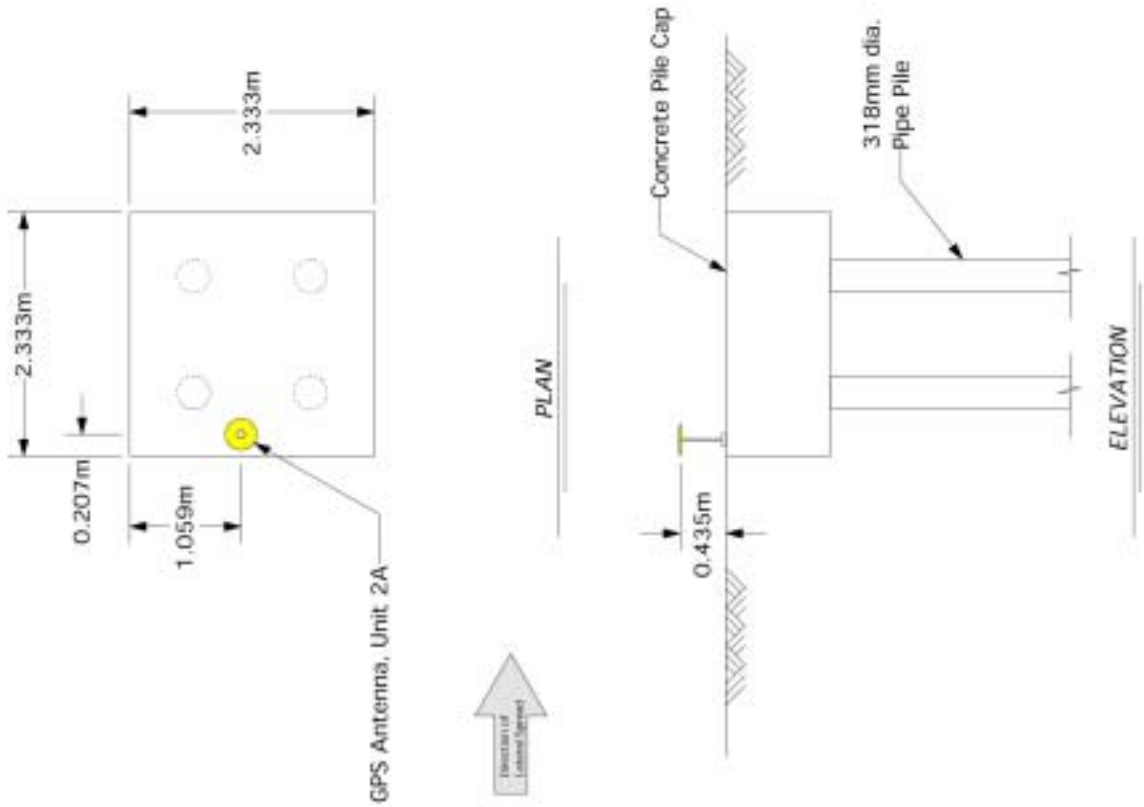

Figure 19 - Position of Unit 2A

Similar to the installation on the 9-pile cap, the GPS antenna for the 4-pile group cap was mounted to the top concrete surface using steel brackets and threaded rod, and the equipment enclosure was secured to the pile cap. A photo of the installation is shown in Figure 20.

Figure 20 – Unit 2A

Unit 2B was positioned approximately 10.4m in front of and in line with the 4-pile group as shown in Figure 21. Similar to the installation of Unit 1C, Unit 2B was affixed to a raft that was tethered to a nearby slope inclinometer casing for

the November test. The mid-height of the antenna was positioned 43.9cm above the raft surface.

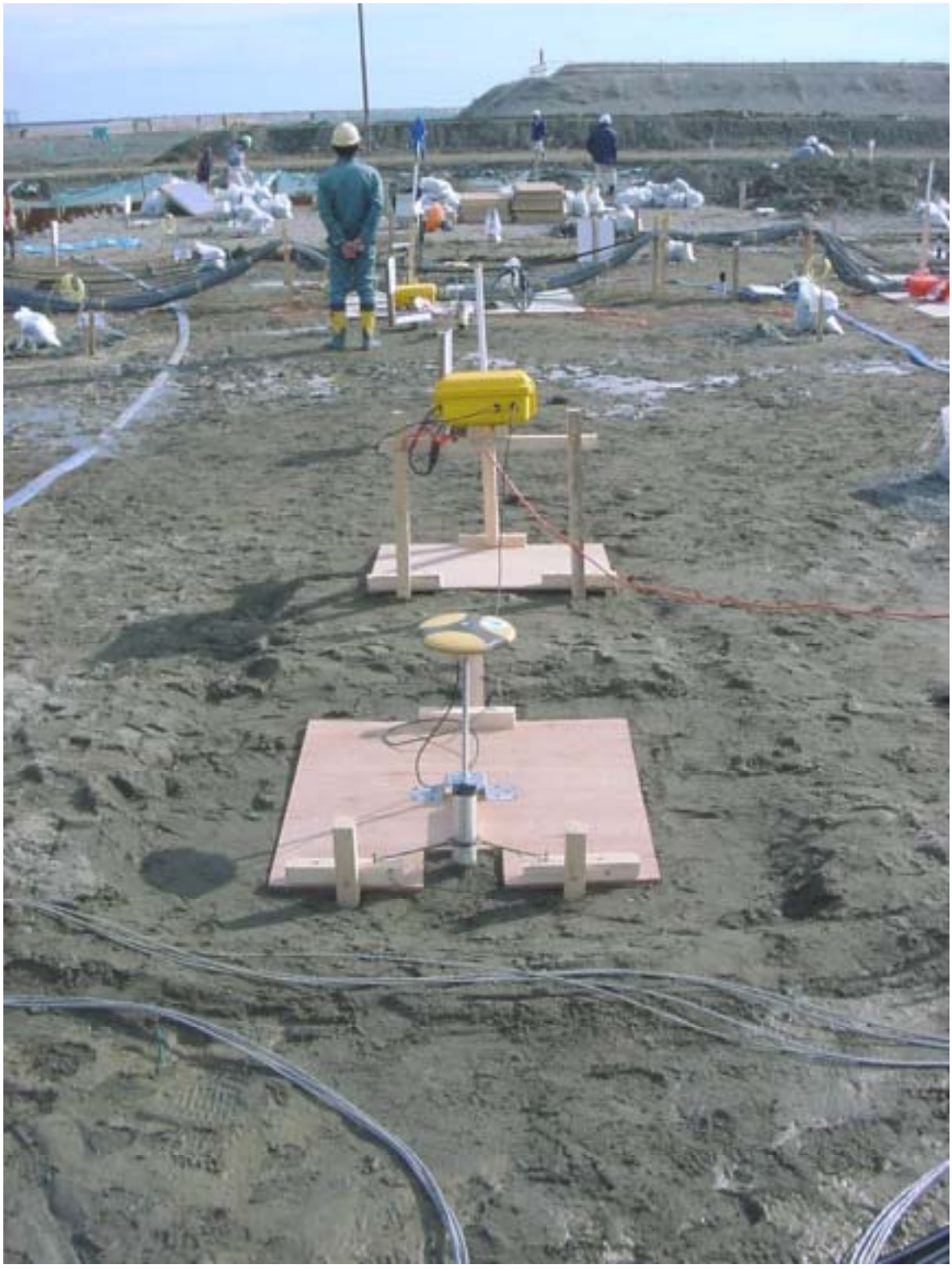

Figure 21 – Unit 2B, November Test

For the December test, the raft was not used, and the GPS antenna was mounted directly to the top of the slope inclinometer casing as shown in Figure 22. The mid-height of the antenna was positioned 79.5cm above the elevation of the surface of the pile cap.

Figure 22 – Unit 2B, December Test

For the November test Units 2D and 2E were installed to measure displacements of the two underground pipeline specimens. Since both utility pipelines were buried below ground, 50mm diameter 1.5m long vertical steel standpipes were welded to the utility pipelines to provide an above ground GPS antenna mount.

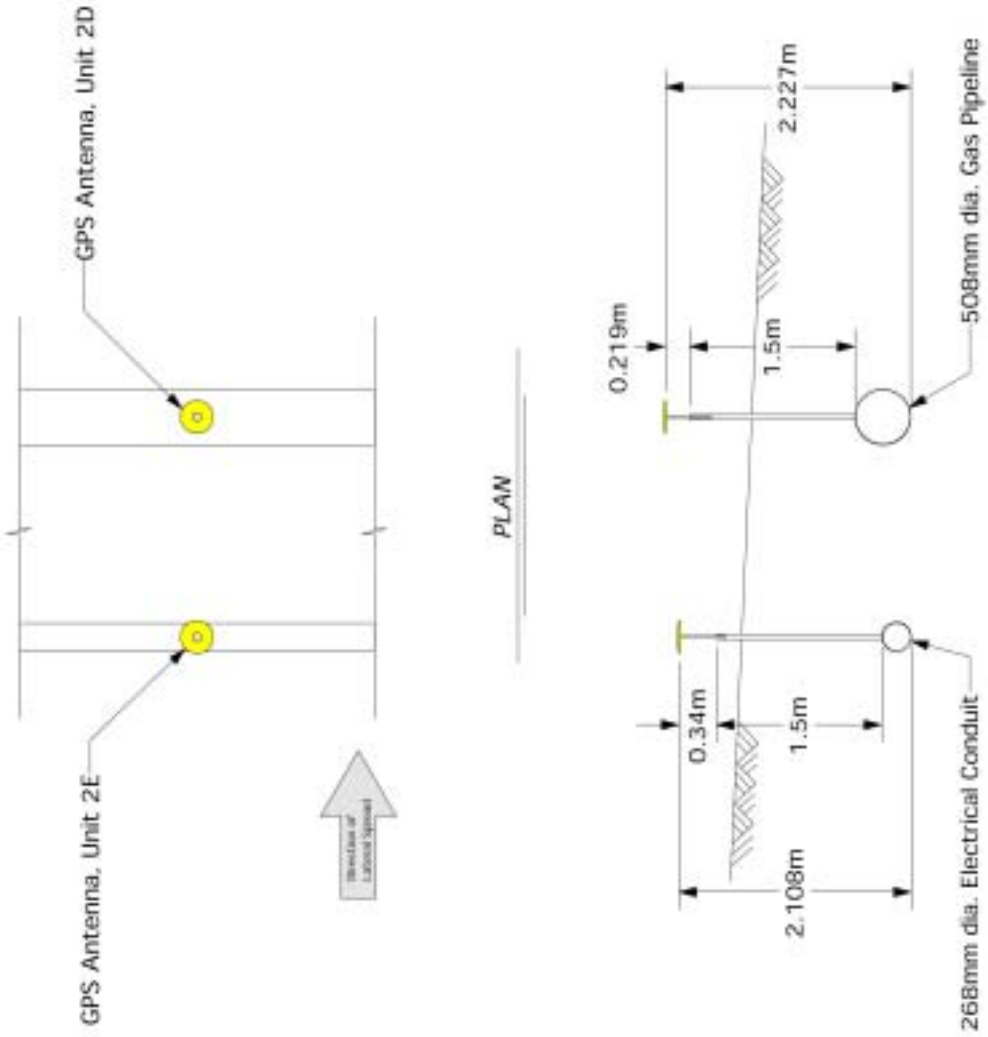

Figure 23 – Units 2D and 2E, November Test

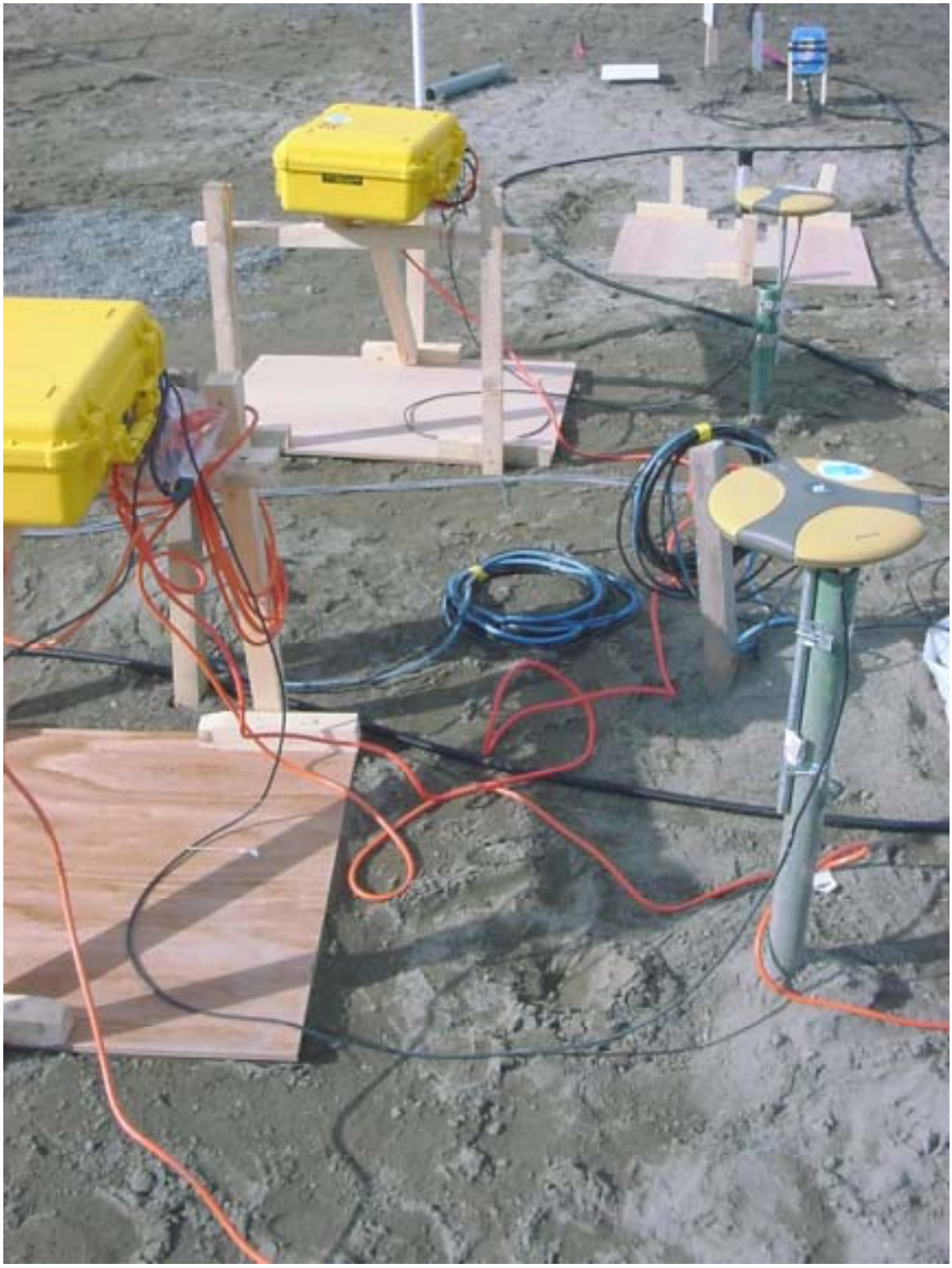

Figure 24 – Units 2D and 2E, November Test

The mid-height of the GPS antennas were 21.9cm and 34.0cm above the tops of the vertical standpipes for Units 2D and 2E, respectively. This configuration allowed above ground measurements for subsurface pipe displacements. Figure 23 provides details on the installation of Units 2D and 2E for the November test. Figure 24 shows a photo from the November test.

For the December test, Unit 2E was removed from the electrical conduit and repositioned on a slope inclinometer casing between the 4-pile group cap and the 9-pile group cap. The mid-height of the GPS antenna was positioned approximately 47.7cm above the ground surface as approximated by the elevation of the surface of the adjacent pile caps. The equipment enclosure was secured to the pile cap for the 4-pile group. Figure 25 shows the position of Unit 2E relative to the adjacent pile groups.

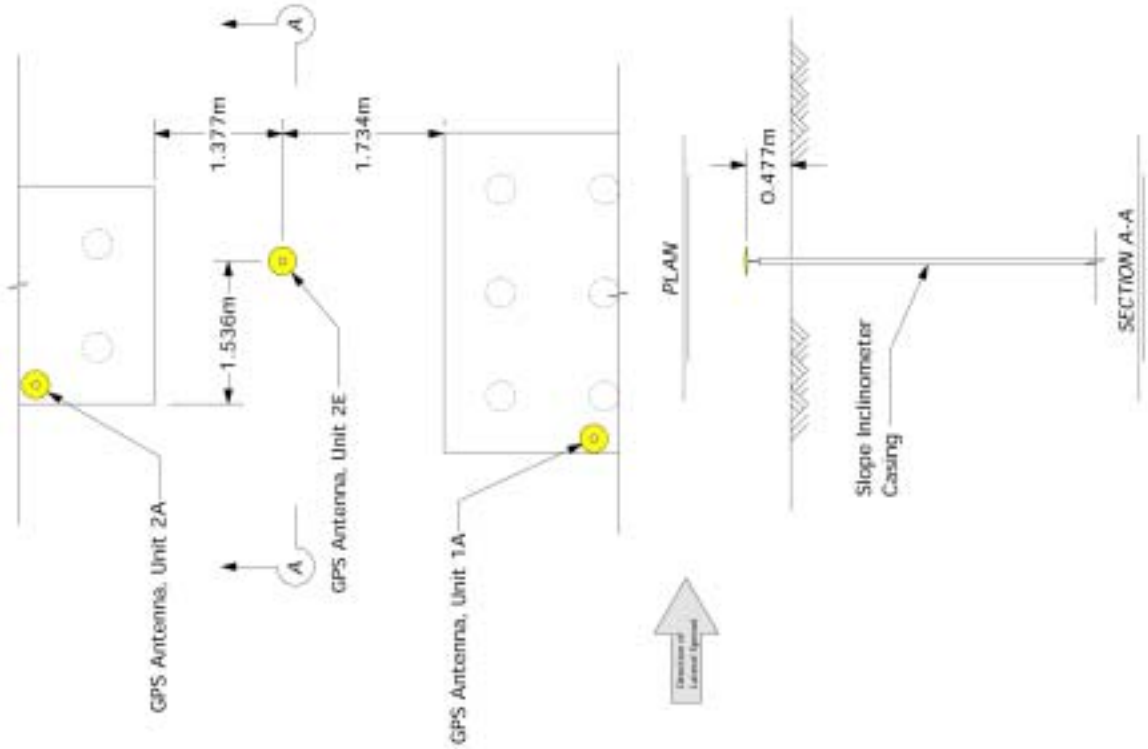

Figure 25 – Unit 2E, December Test

2.4 Monitoring Center

A monitoring center was established approximately 100m away from the blast zone in a temporary trailer office. The monitoring center provided a safe offsite environment for Caltrans staff to observe the test during blasting while monitoring the processing status of the GPS field units. A photo of the monitoring center is shown in Figure 26.

Two base stations were utilized to process the data from the ten field units. Each base station unit was comprised of a GPS receiver and antenna, five wireless data transceivers, and a laptop computer with the RTK-GPS processing software. These components were packaged in a large weatherproof enclosure as shown in Figure 27. A single base station unit could have been used to capture the data for all ten field units, however, the quantity of data recorded would have taxed the capabilities of the laptop computer. As such, two systems were used, splitting the processing and data logging tasks between them.

The GPS antennas for the two base stations were mounted to the tops of steel poles affixed to the roof of the trailer. This location was chosen to limit potential multipath and line-of-sight errors resulting from nearby steel scaffolding. Additional guy wires and bracing were used to stabilize the poles from wind and other vibration sources. The antennas for the wireless transceivers were also mounted to the pole and provided good line-of-sight with the field units.

Figure 26 – Monitoring center trailer

Figure 27 – Monitoring center unit

2.5 Creating the Lateral Spread

The ground deformations associated with lateral spread were created by using explosives to induce liquefaction throughout the test site. In preparation for both the November and December tests, a Japanese blasting contractor installed multiple explosives in vertically drilled holes spaced at 6.0m on centers in a regular grid pattern throughout the test site as shown in Figure 28. Two explosive charges were placed in each of the blast holes, shallow charges at elevation –0.500m and deeper charges at elevation –4.500m.

Figure 28 – Placing explosives

The blasting sequence was planned such that the explosives at the back corner of the site, farthest from the waterway, would be detonated initially. Blasting proceeded sequentially to adjacent holes in the same row and then moved to the next row proceeding towards the front of the site as shown in Figure 29.

Secondary additional explosives were placed around the perimeter of the test site adjacent to the surrounding sheet pile wall for the November test. These explosives were detonated following the initial blast sequence within the test area. These explosives were designed specifically to break the tie back rods, thus allowing more displacement throughout the site. Sets of tertiary explosives were placed adjacent to the steel tie back rods for the quay wall. These explosives were designed specifically to cause a structural failure of the quay wall. Since the quay wall was expected to effectively retain the liquefied soil following the primary and secondary blasts, the tertiary blasting was necessary to fail the wall to allow the soil to displace beyond the limits of the test area.

For the December test, the sheet pile walls were removed and, as such, additional blasting around the perimeter was not necessary. However, an additional row of explosives were placed on the steeper 2:1 slope between the pile groups and the waterway. These explosives were intended to loosen the toe of the sloped test site to encourage displacements similar to a theoretical infinite slope failure.

These explosives were detonated approximately 15 seconds prior to initiating the full blasting sequence.

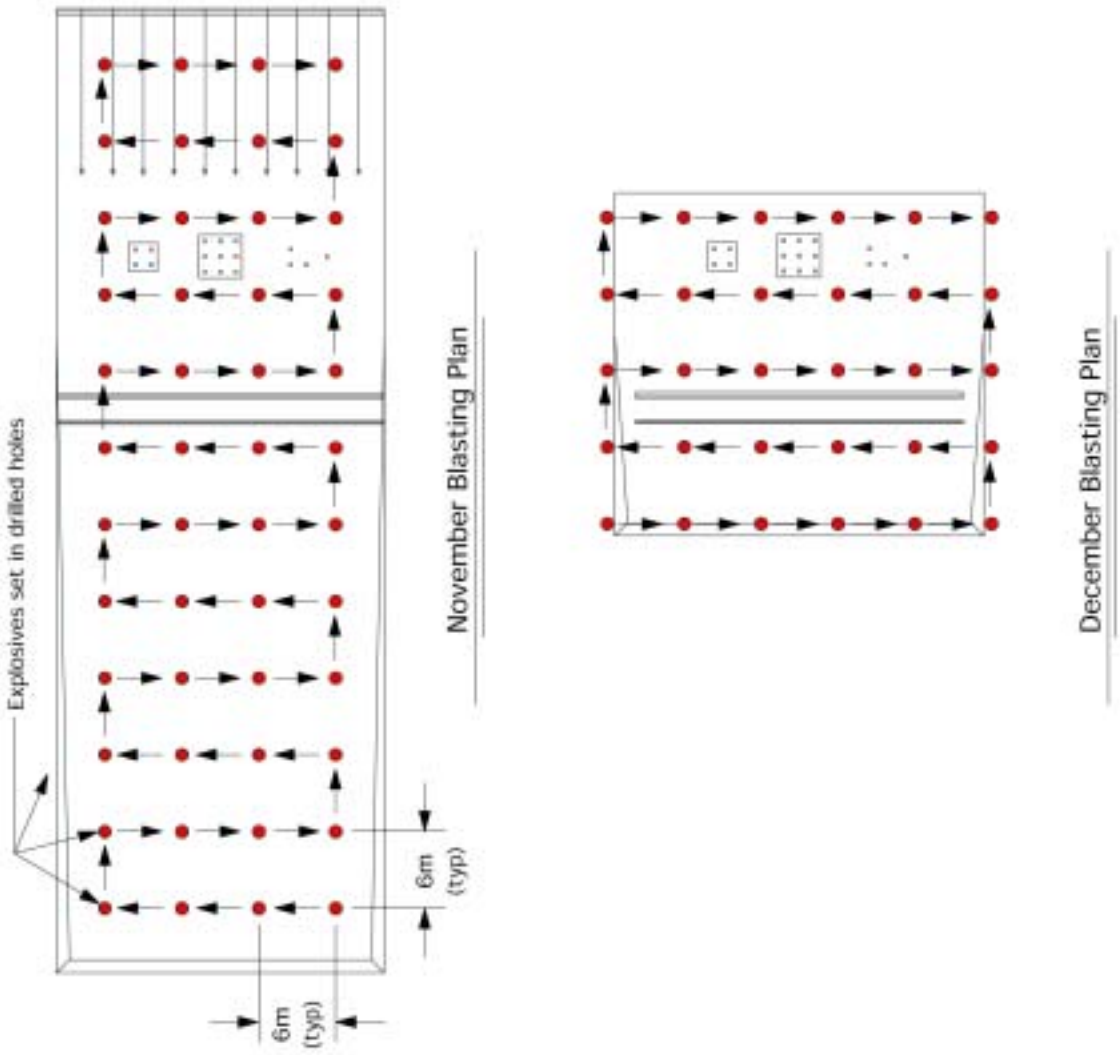

Figure 29 – Blasting plans

Blasting took place on November 13, 2001. The weather was ideal that day with clear skies and temperatures ranging from 0ºC to 10ºC throughout the day. Additional measures were taken the night before the test to improve the probability of successfully liquefying the site and generating lateral spread. This included wetting the site using a series of soaker hoses placed on the ground across the site. Over 400 visitors were present to observe the test, including test sponsors as well as representatives from industry and academic institutions from Japan and the United States.

The primary blast sequence commenced at approximately 2:26:24.30 PM local time (192384.30 GPS time), and proceeded over a period of approximately 36 seconds. Figures 30 and 31 show photos of the site during primary blasting. The secondary explosives were detonated after roughly 6 seconds following the completion of the primary blast sequence. The tertiary explosives near the quay wall were detonated approximately 44 seconds later. Figure 32 shows a photo of the blasting near the quay wall.

Figure 30 – Blasting underway, November Test

QuickTime™ and a
DV - NTSC decompressor
are needed to see this picture.

QuickTime™ and a
DV - NTSC decompressor
are needed to see this picture.

QuickTime™ and a
DV - NTSC decompressor
are needed to see this picture.

QuickTime™ and a
DV - NTSC decompressor
are needed to see this picture.

Figure 31 – Blasting underway, November Test

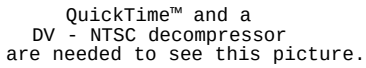

Figure 32 – Blasting near the quay wall, November Test

The second test took place on December 14, 2001. The execution of the second test was made challenging due to heavy snowfall, temperatures between –10ºC and 0ºC, and record setting 100kph winds on the day of the test. Ground freeze became an issue since frozen soil is not liquefiable nor conducive to lateral spread. Based upon driving steel stakes throughout sections of the site, the ground freeze was estimated to be approximately 20 to 30cm. As such, on the morning of the test, construction crews used jackhammers to break up the frozen ground surface in an area 3 to 5m buffering the pile groups as shown in Figure 33.

Figure 33 – Jackhammer operation to break up frozen soil surface

The primary blast sequence commenced at approximately 2:16:41.00 PM local time (451001.00 GPS time), and proceeded over a period of approximately 15 seconds. Approximately 19 seconds prior to the primary blast sequence, the explosives near the toe of the slope and the waterway were detonated. Figure 34 shows a photo during the blasting.

Figure 34 – Blasting underway, December Test

3.0 Measurements From the Tests in Japan

3.1 Data Collection and Processing

Raw GPS data was transmitted from the GPS field units back to the monitoring center where it could be processed in real time and logged by the two laptop computers. Multiple sets of data, both raw and processed, were collected for each test including positioning data before the blast, during the blast, immediately following the blast, and the following day. Other data sets were collected such as a survey of the test site to determine the relative positions of the base and field GPS antennas in the local grid system. All data was processed on the laptop computers in real time using the software application *RTKNav 3.0* (Waypoint 2000).

Two types of data files were created by the processing software, RTKNav, for each GPS field unit during the logging process: a raw data file, designated by the suffix *LOG*, and a processed data file, designated by the suffix *OUT*. The LOG file contains fundamental GPS satellite information, such as the position, doppler, and phase measurements from each satellite. The LOG file is useful in the event that the measurements need to be reprocessed. The OUT file contains the processed positioning information including precise GPS time, horizontal coordinates, height, and additional parameters used to assess the measurement quality.

For all data sets, positioning information was collected at a rate of 10Hz. Although 20Hz positioning data was possible from the GPS equipment, the higher data rates and increased throughput requirements could not be supported by the 900MHz spread spectrum wireless transceivers. At 10Hz, LOG files were created at a rate of approximately 3.5KB/sec for each GPS receiver. For 10 receivers over a typical 20 minute logging session, over 40MB were logged. A single OUT file over the same time period for 10 receivers at 10Hz totaled approximately 15MB.

Static GPS antenna positions prior to and following the blasting were determined from data sets collected over periods of approximately 15 minutes or longer. Shorter data sets of 2 to 5 minutes were used to determine positions immediately following blasting. GPS antennas were stationary during these measurements and 10Hz data was collected under ideal surveying conditions. Raw measurements were selectively filtered to include only the highest quality measurements. These were measurements where the GPS satellite constellation and orientation were ideal, the signal strength high, and carrier phase ambiguities readily determined. These parameters were combined into a single parameter, *quality factor*, and reported by the processing software for each measurement. On average 91% of all of the collected measurements met the criteria for the highest quality factor.

Static positions were determined by calculating the statistical average of the data set using the selected measurements. These accuracy of the measurements were consistent with expected accuracies for RTK-GPS processing techniques with a mean horizontal standard deviation of 3mm and a mean vertical standard deviation of 7mm. The mean standard deviations were determined from the distribution of standard deviations calculated for each field unit from each data set and are provided in Tables 3 through 6.

Field Unit	Standard Deviation of Position Measurements		
	Easting (m)	Northing (m)	Height (m)
1A	0.003	0.003	0.009
1B	0.003	0.003	0.007
1C	0.003	0.004	0.007
1D	0.003	0.004	0.007
1E	0.003	0.003	0.009
2A	0.003	0.003	0.007
2B	0.002	0.003	0.005
2C	0.003	0.003	0.007
2D	0.003	0.003	0.006
2E	0.004	0.004	0.006

Table 3 – November 13, 2001, Pre-Blast Data Set Statistics

Field Unit	Standard Deviation of Position Measurements		
	Easting (m)	Northing (m)	Height (m)
1A	0.002	0.003	0.006
1B	0.002	0.003	0.004
1C	0.003	0.004	0.007
1D	0.003	0.004	0.008
1E	0.004	0.004	0.009
2A	0.004	0.004	0.009
2B	0.000	0.001	0.004
2C	0.000	0.001	0.004
2D	0.003	0.004	0.009

2E	0.004	0.005	0.013

Table 4 – November 13, 2001, Post-Blast Data Set Statistics

Field Unit	Standard Deviation of Position Measurements		
	Easting (m)	Northing (m)	Height (m)
1A	0.001	0.003	0.005
1B	0.002	0.002	0.005
1C	0.002	0.002	0.005
1D	0.002	0.003	0.005
1E	0.003	0.002	0.006
2A	0.002	0.002	0.004
2B	0.003	0.002	0.003
2C	0.003	0.002	0.003
2D	0.002	0.002	0.002
2E	0.002	0.002	0.003

Table 5 – December 14, 2001, Pre-Blast Data Set Statistics

Field Unit	Standard Deviation of Position Measurements		
	Easting (m)	Northing (m)	Height (m)
1A	0.002	0.004	0.010
1B	0.002	0.003	0.010
1C	0.002	0.003	0.011
1D	0.003	0.003	0.013
1E	0.003	0.006	0.009
2A	0.003	0.004	0.008
2B	0.002	0.003	0.008
2C	0.002	0.003	0.009
2D	0.002	0.003	0.008
2E	0.002	0.004	0.010

Table 6 – December 14, 2001, Post-Blast Data Set Statistics

Tables 7 through 10 summarize the results of the pre-blast and post-blast static surveys. Data in the table includes the horizontal northing and easting coordinate as well as height, reported in units of meters in a local grid system established by the test organizers. Changes in the position of the GPS antennas are tabulated in terms of total vector displacement as well as individual

horizontal and vertical components. Positioning data is provided for measurements just before the blast, within minutes following the blast, and the day after the blast.

	PreBlast	(192300 GPS Time)		Post Blast	(192455 GPS Time)		Total Vector	Horizontal	Vertical
Location	X (east)	Y (north)	Z (elev)	X (east)	Y (north)	Z (elev)	Displacement (m)	Displacement (m)	Displacement (m)
1A (9-pile group)	162.266	-166.999	0.199						
1B (9-pile near)	160.677	-166.265	0.276						
1C (9-pile free)	156.153	-163.386	0.333	156.445	-163.563	0.332	0.342	0.342	-0.001
1D (1-pile)	159.610	-175.214	0.440	159.936	-175.377	0.446	0.365	0.365	0.006
1E (1-pile SI)	158.758	-174.646	0.330						
2A (4-pile group)	165.535	-161.938	0.201	165.708	-162.069	0.215	0.217	0.217	0.014
2B (free field)	156.265	-156.773	0.398						
2C (3-pile group)	160.374	-172.311	1.505	160.857	-172.579	1.515	0.552	0.552	0.011
2D (gas pipe)	154.089	-162.367	0.742	154.378	-162.607	0.731	0.376	0.376	-0.011
2E (electric pipe)	152.264	-161.349	0.617	152.548	-161.601	0.574	0.382	0.380	-0.043

Table 7 – Pre-blast and Post-Blast Positions, November Test, approximately 3 minutes following blasting

	PreBlast	(192300 GPS Time)		Post Blast	(271840 GPS Time)		Total Vector	Horizontal	Vertical
Location	X (east)	Y (north)	Z (elev)	X (east)	Y (north)	Z (elev)	Displacement (m)	Displacement (m)	Displacement (m)
1A (9-pile group)	162.266	-166.999	0.199	162.403	-167.117	0.213	0.182	0.181	0.013
1B (9-pile near)	160.677	-166.265	0.276	160.916	-166.417	0.308	0.285	0.283	0.032
1C (9-pile free)	156.153	-163.386	0.333	156.439	-163.554	0.243	0.344	0.332	-0.090
1D (1-pile)	159.610	-175.214	0.440	159.923	-175.370	0.448	0.350	0.350	0.008
1E (1-pile SI)	158.758	-174.646	0.330	159.057	-174.804	0.356	0.340	0.339	0.026
2A (4-pile group)	165.535	-161.938	0.201	165.705	-162.065	0.206	0.212	0.212	0.005
2B (free field)	156.265	-156.773	0.398	156.529	-157.009	0.307	0.365	0.354	-0.091
2C (3-pile group)	160.374	-172.311	1.505	160.854	-172.573	1.517	0.548	0.547	0.012
2D (gas pipe)	154.089	-162.367	0.742	154.375	-162.603	0.631	0.387	0.371	-0.111
2E (electric pipe)	152.264	-161.349	0.617	152.550	-161.605	0.489	0.405	0.384	-0.128

Table 8 – Pre-blast and Post-Blast Positions, November Test, approximately 22 hours following blasting

	PreBlast	(450960 GPS Time)		Post Blast	(451040 GPS Time)		Total Vector	Horizontal	Vertical
Location	X (east)	Y (north)	Z (elev)	X (east)	Y (north)	Z (elev)	Displacement (m)	Displacement (m)	Displacement (m)
1A (9-pile group)	162.408	-167.121	0.205	162.536	-167.212	0.214	0.157	0.157	0.009
1B (9-pile near)	160.845	-166.486	0.436	160.971	-166.570	0.502	0.165	0.151	0.066
1C (9-pile free)	156.121	-163.256	0.565	156.272	-163.388	0.580	0.201	0.200	0.015
1D (1-pile)	159.962	-175.389	0.436	160.229	-175.523	0.438	0.299	0.299	0.002
1E (1-pile SI)	158.994	-174.872	0.298	159.219	-174.928	0.308	0.232	0.232	0.010
2A (4-pile group)	165.700	-162.061	0.213	165.857	-162.156	0.222	0.184	0.184	0.009
2B (free field)	156.049	-156.776	0.366	156.122	-156.858	0.394	0.113	0.110	0.028
2C (3-pile group)	160.901	-172.590	1.506	161.322	-172.806	1.487	0.474	0.474	-0.020
2D (gas pipe)	154.375	-162.619	0.440	154.517	-162.715	0.333	0.202	0.171	-0.107
2E (between caps)	165.662	-165.026	0.242	166.049	-165.246	0.227	0.446	0.445	-0.015

Table 9 – Pre-blast and Post-Blast Positions, December Test, approximately 1.3 minutes following blasting

Location	PreBlast (450960 GPS Time) X (east)	Y (north)	Z (elev)	Post Blast (525076 GPS Time) X (east)	Y (north)	Z (elev)	Total Vector Displacement (m)	Horizontal Displacement (m)	Vertical Displacement (m)
1A (9-pile group)	162.408	-167.121	0.205	162.530	-167.210	0.204	0.151	0.151	-0.001
1B (9-pile near)	160.845	-166.486	0.436	160.970	-166.569	0.483	0.157	0.150	0.047
1C (9-pile free)	156.121	-163.256	0.565	156.277	-163.375	0.556	0.196	0.196	-0.009
1D (1-pile)	159.962	-175.389	0.436	160.230	-175.515	0.421	0.297	0.297	-0.014
1E (1-pile SI)	158.994	-174.872	0.298	159.218	-174.926	0.286	0.231	0.230	-0.012
2A (4-pile group)	165.700	-162.061	0.213	165.842	-162.158	0.220	0.173	0.173	0.007
2B (free field)	156.049	-156.776	0.366	156.121	-156.864	0.410	0.122	0.114	0.044
2C (3-pile group)	160.901	-172.590	1.506	161.325	-172.804	1.482	0.476	0.475	-0.024
2D (gas pipe)	154.375	-162.619	0.440	154.515	-162.716	0.296	0.223	0.170	-0.145
2E (between caps)	165.662	-165.026	0.242	166.066	-165.244	0.220	0.460	0.460	-0.021

Table 10 – Pre-blast and Post-Blast Positions, December Test, approximately 20 hours following blasting

Measurements were collected as blasting progressed to track the dynamic motions of the GPS antennas resulting from the immediate blast and subsequent lateral spread. As with the static survey, the dynamic data was also collected at 10Hz and processed in real-time. Figures 35 through 50 provide the time history of displacements for lateral, transverse, and vertical components as well as a plot of the complete displacement path in the horizontal plane. For the time history plots, *GPS time* is indicated on the primary axis. GPS time is measured as the cumulative seconds in a single GPS week relative to the global time standard, Coordinated Universal Time (UTC). The time history records shown in Figures 35 through 40 for the November test represent GPS times 192370.0 to 192450.0, or 2:26:10.0 PM to 2:27:30.0 PM local time in Japan. The time history records shown in Figures 41 through 50 for the December test represent GPS times 450960.0 to 451040.0, or 2:16:00.0 PM to 2:17:20.0 PM local time in Japan.

Some data loss occurred during the critical blasting period due to intermittent GPS antenna interference and wireless communications loss. For the November test loose soil at the surface was thrown in the air by the blasting and was suspected to have generated much of the interference. Consequently, in four of the ten records (Units 1A, 1B, 1E, and 2B), the periods of time during the blasting were not captured at all. In two of the six records obtained, there were short periods of data loss of about 5 seconds. For the December test there was significantly less debris thrown in the air since the ground was frozen. Although

there was significant snowfall at the time of the test, GPS satellite signals at 1227.60 MHz and 1575.42 MHz and wireless transceiver signals in the 902 to 928 Mhz band appeared to be relatively unaffected by the snowfall.

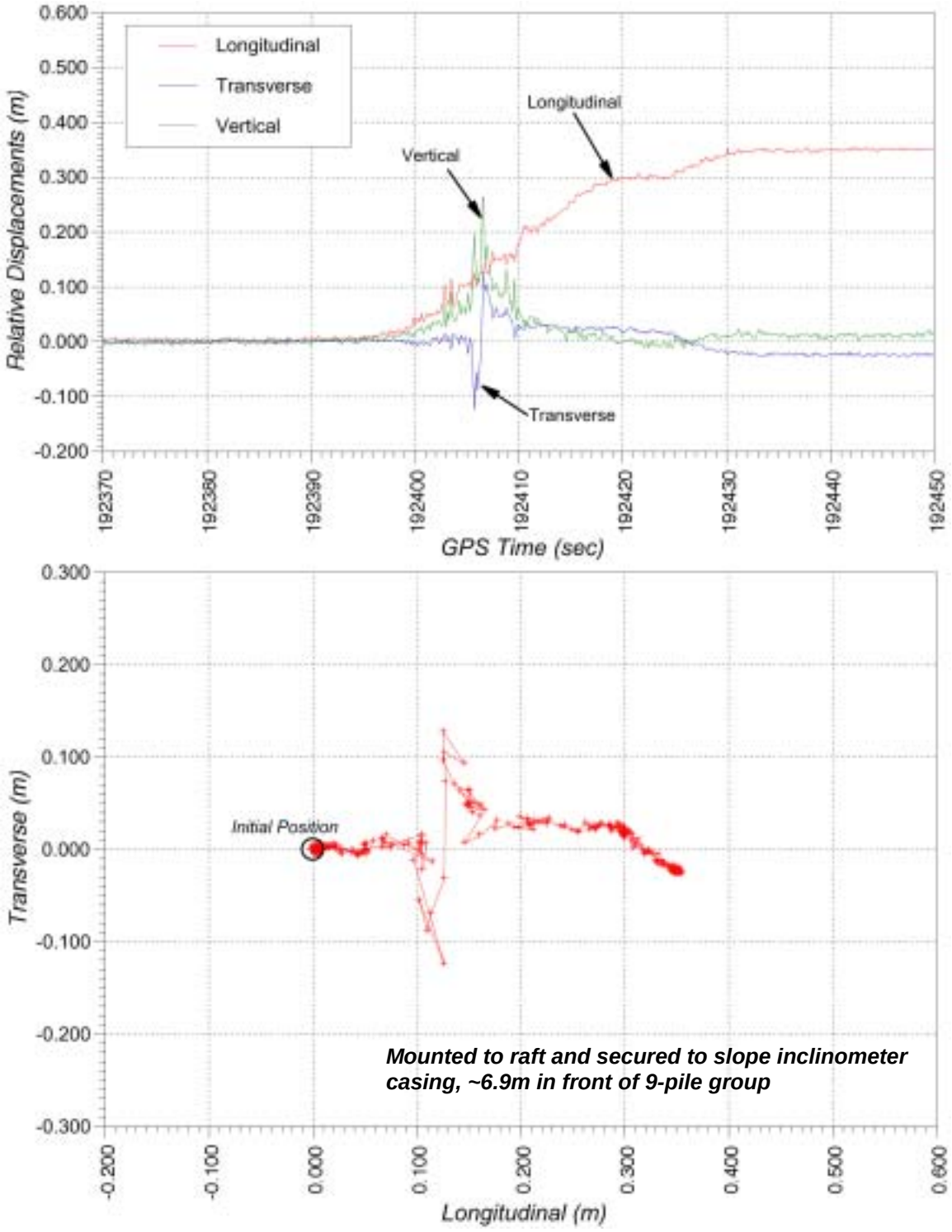

Figure 35 – Time-history record and plot for Unit 1C, November Test

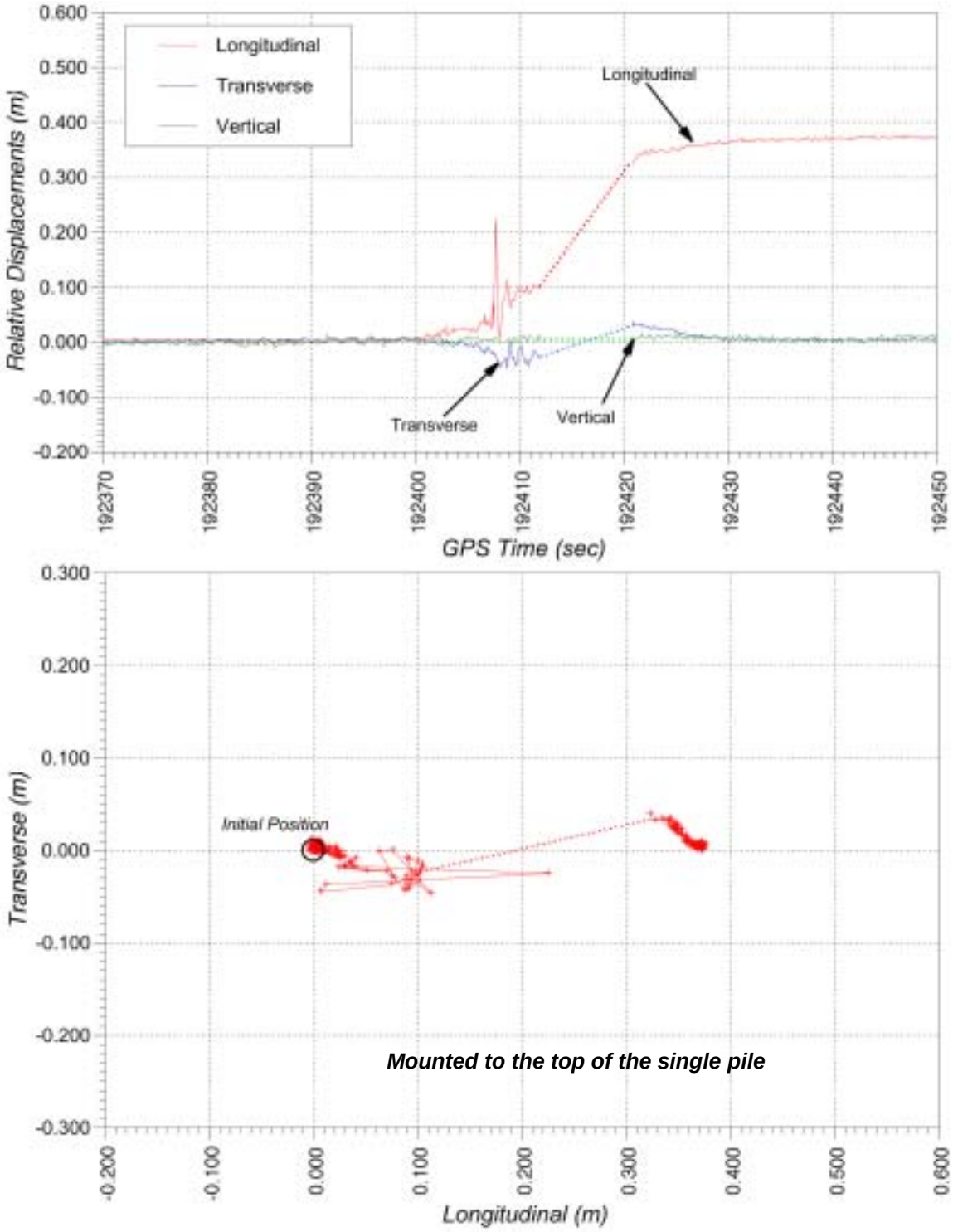

Figure 36 – Time-history record and plot for Unit 1D, November Test

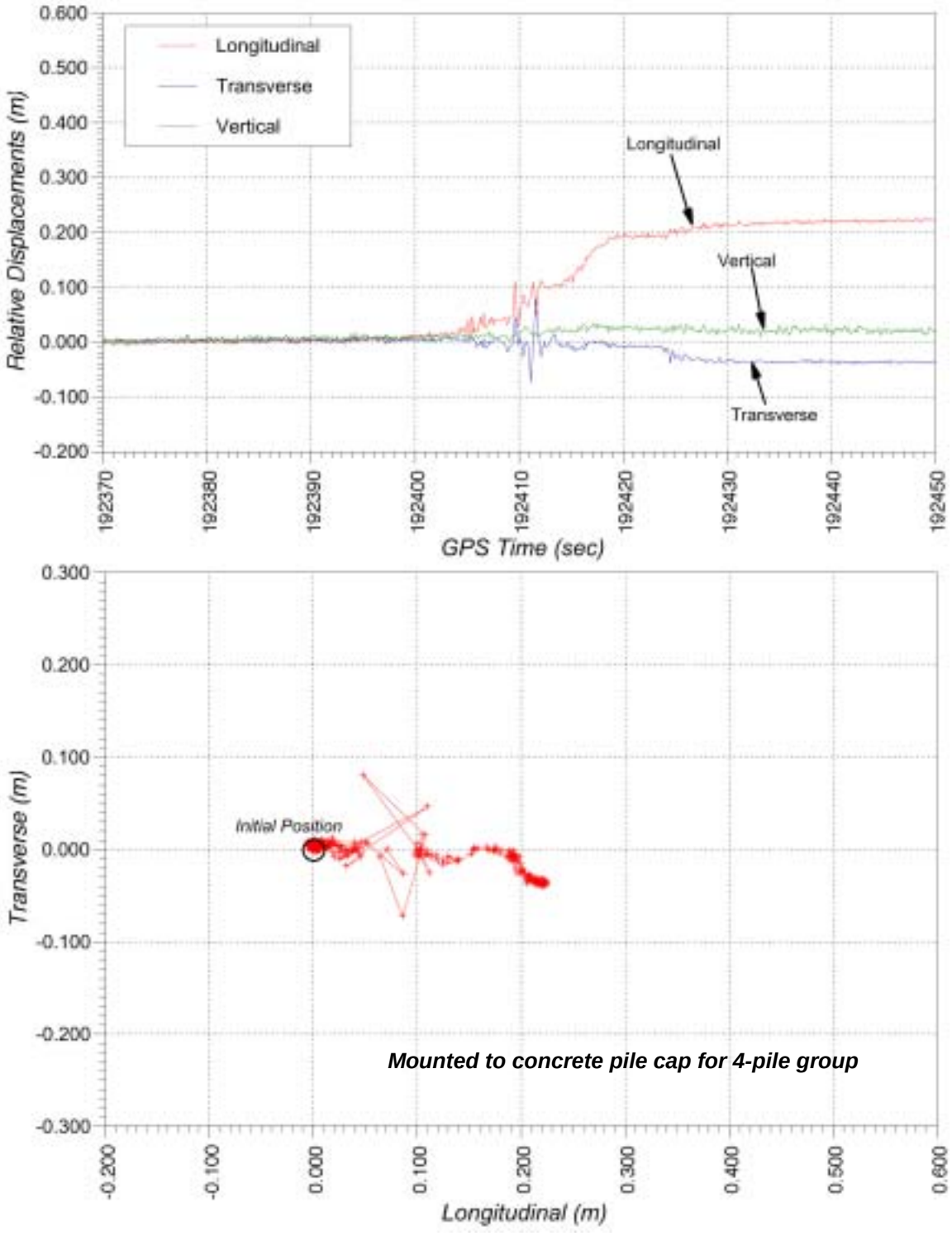

Figure 37 – Time-history record and plot for Unit 2A, November Test

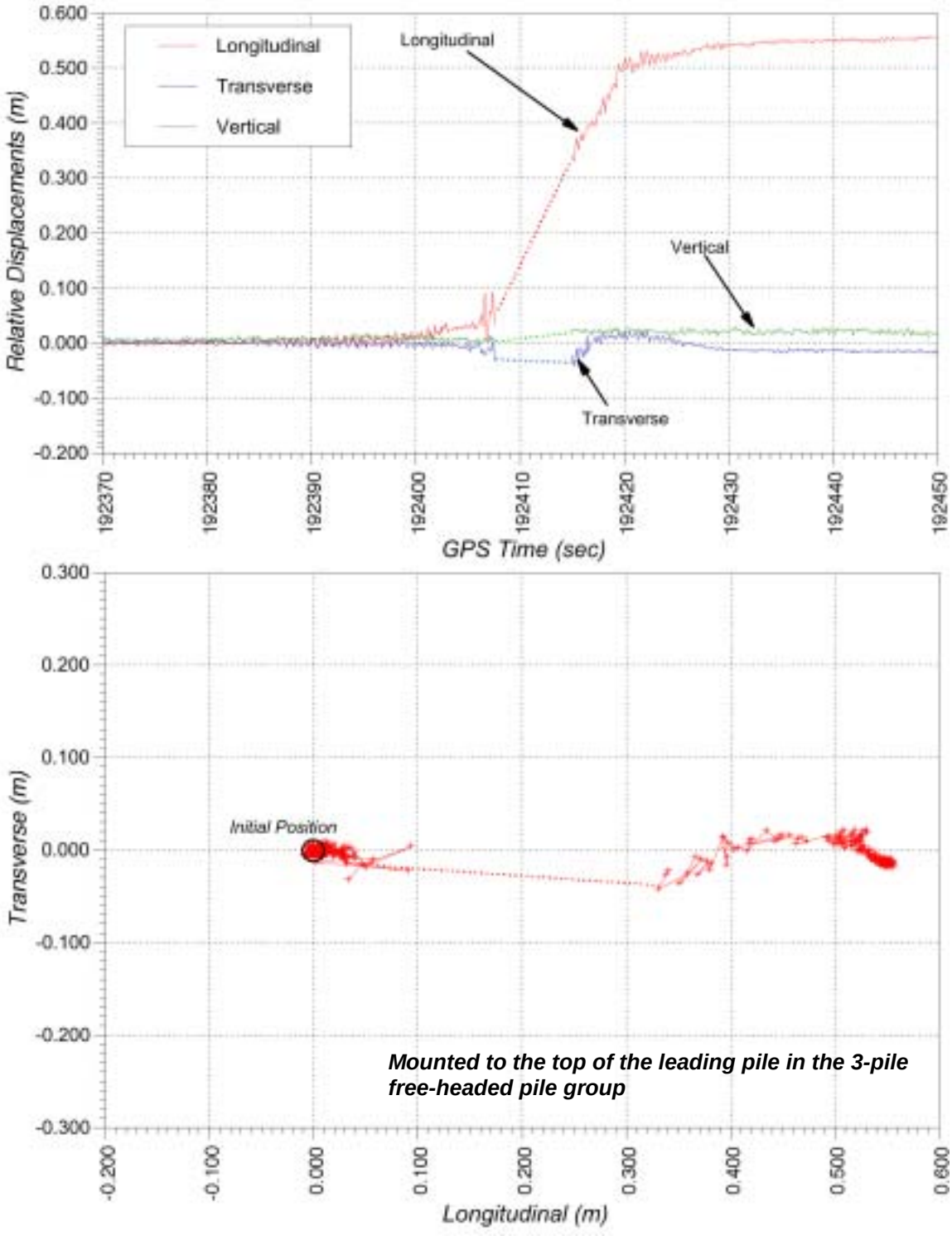

Figure 38 – Time-history record and plot for Unit 2C, November Test

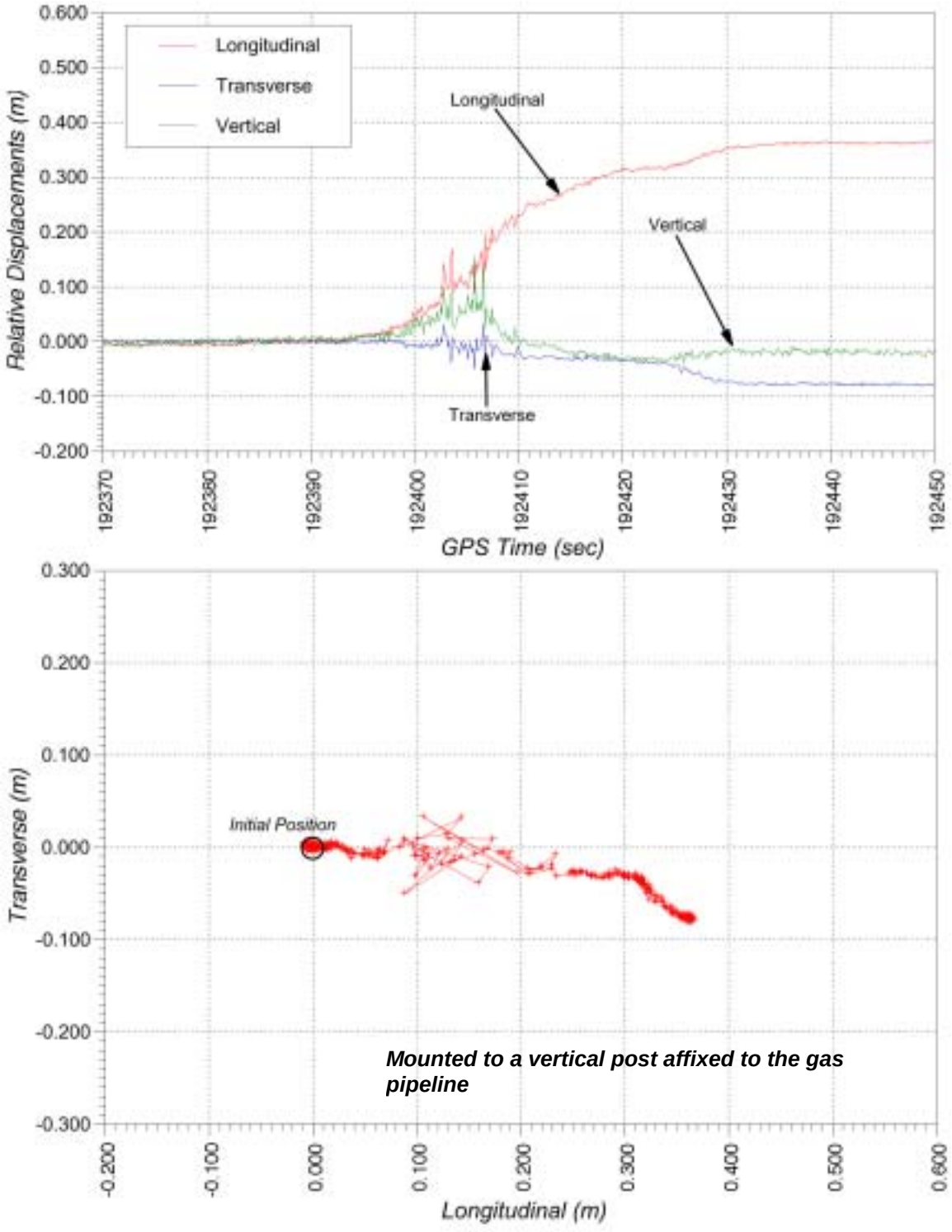

Figure 39 – Time-history record and plot for Unit 2D, November Test

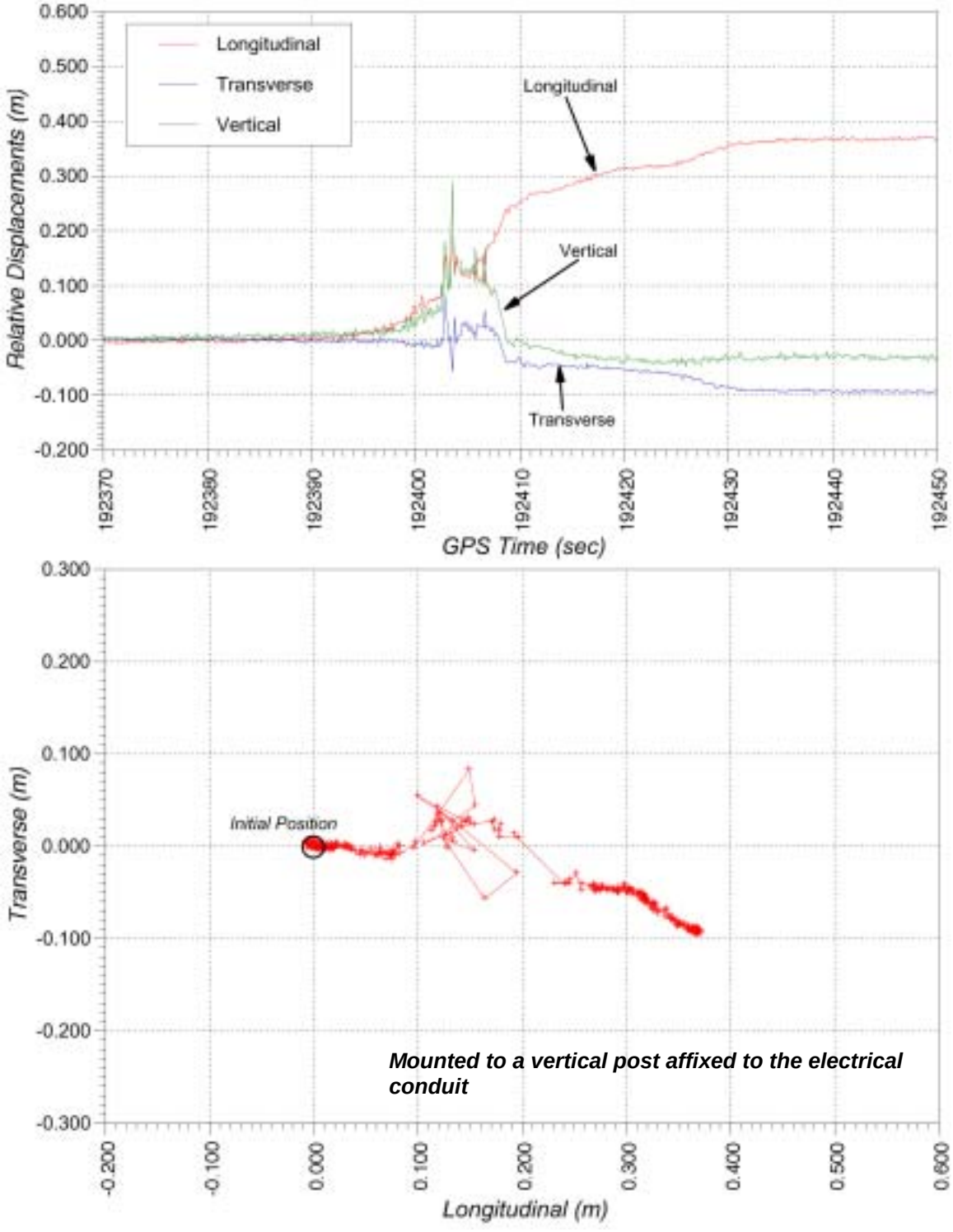

Figure 40 – Time-history record and plot for Unit 2E, November Test

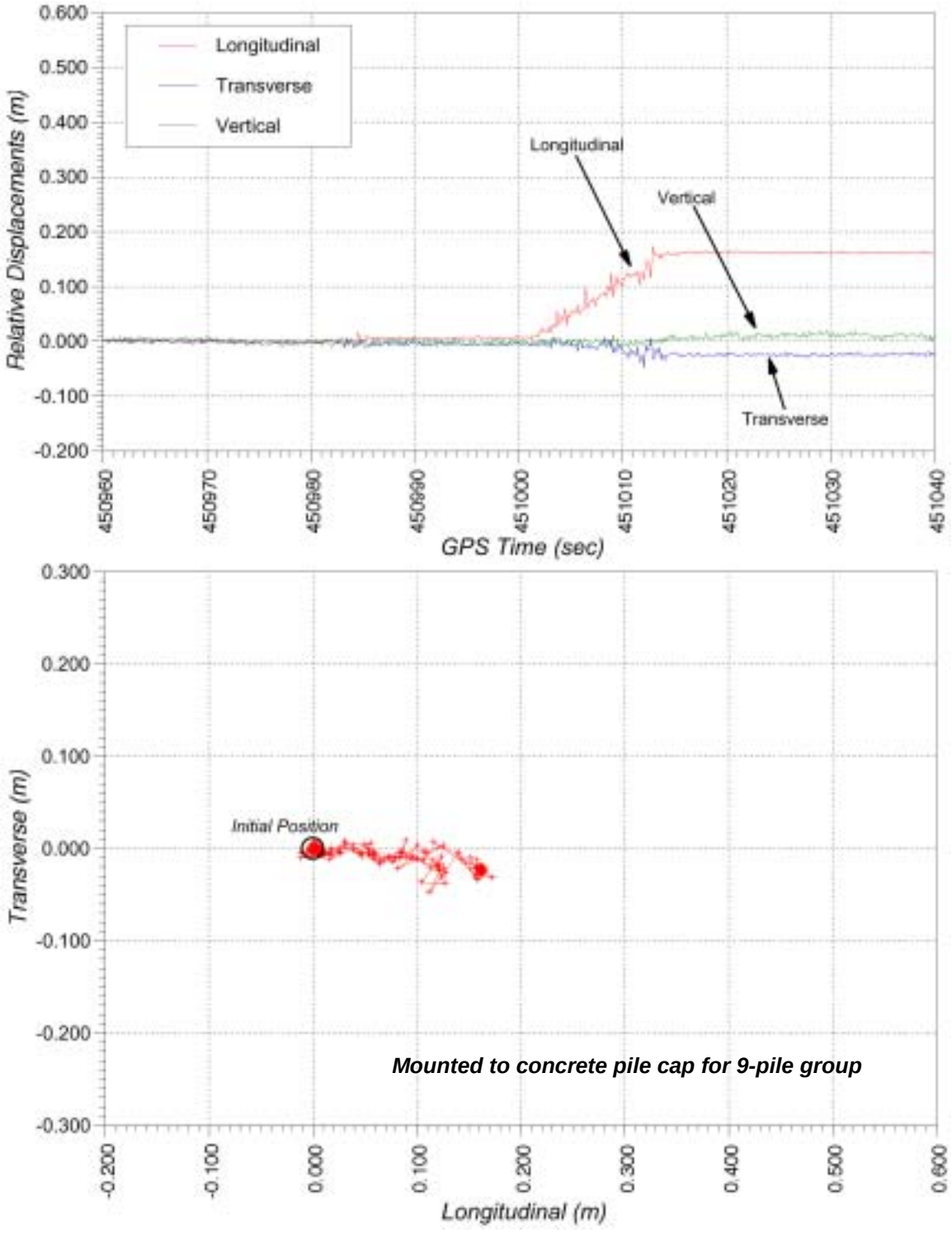

Figure 41 – Time-history record and plot for Unit 1A, December Test

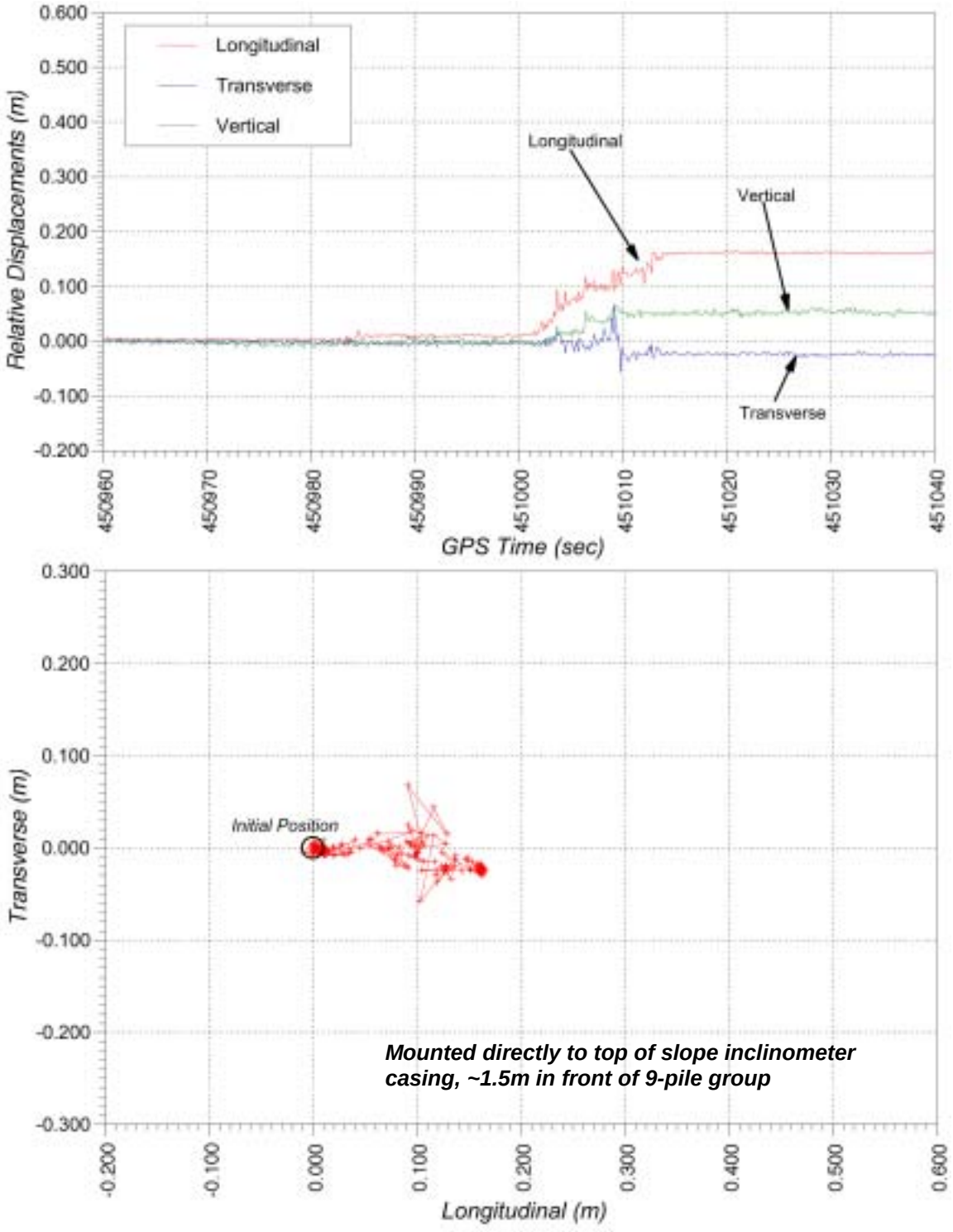

Figure 42 – Time-history record and plot for Unit 1B, December Test

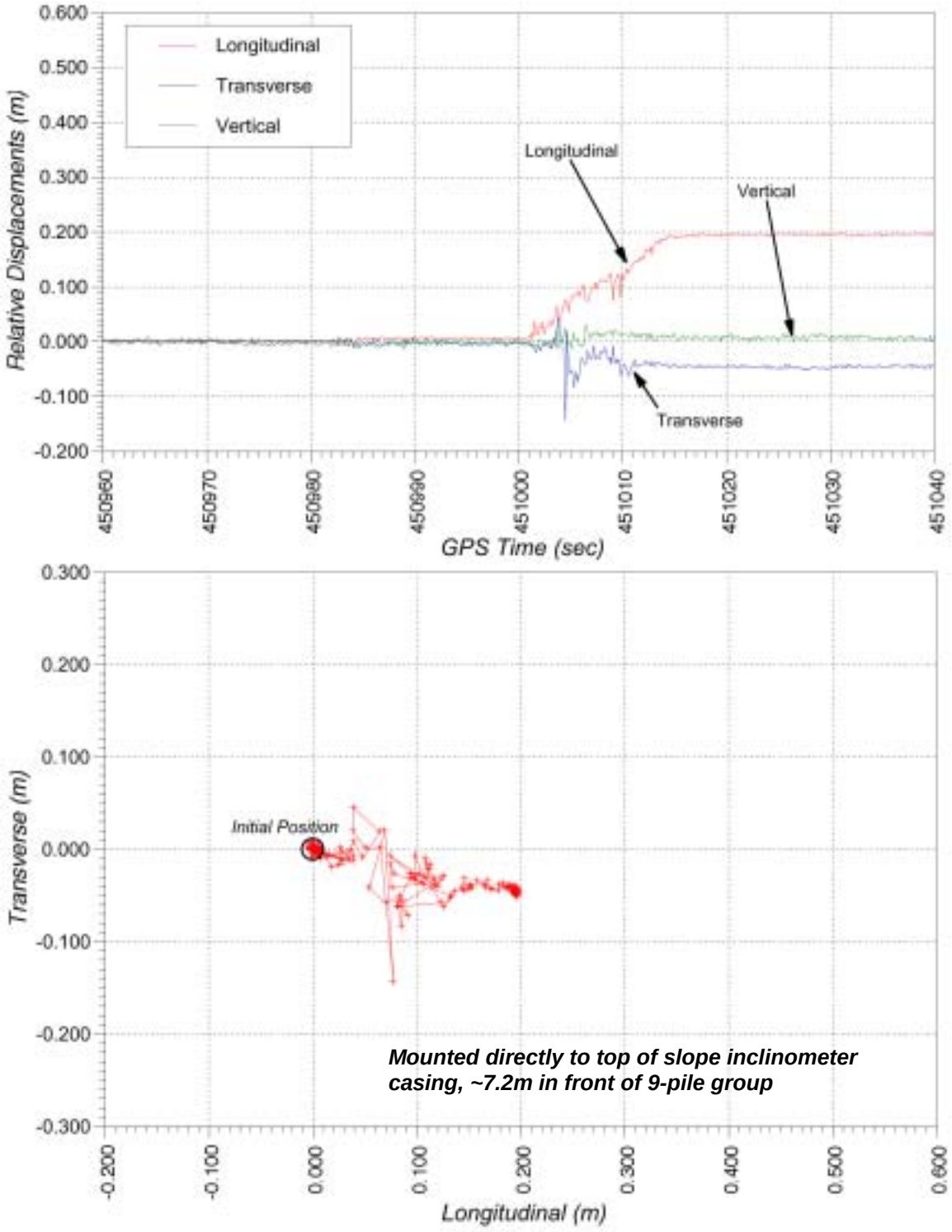

Figure 43 – Time-history record and plot for Unit 1C, December Test

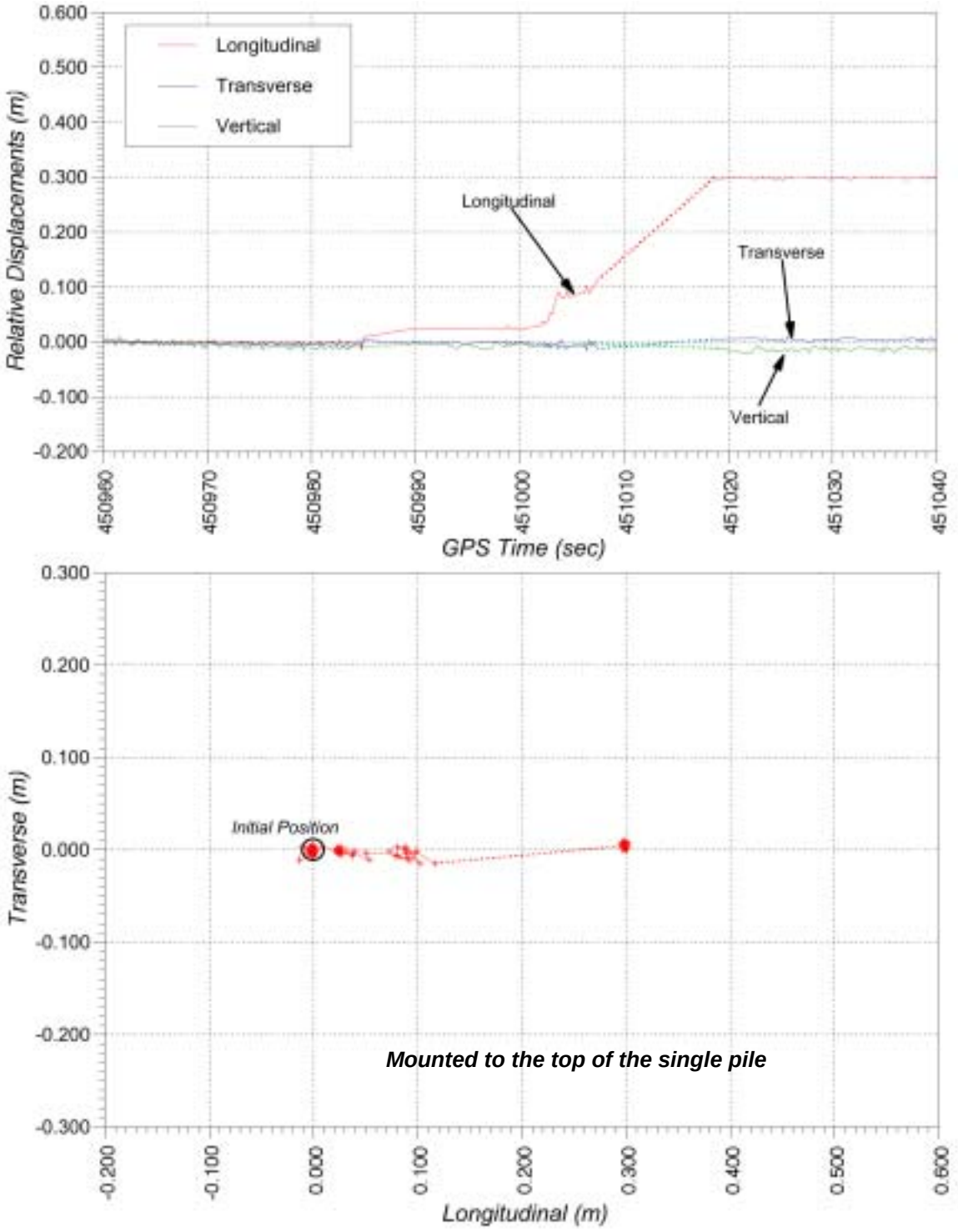

Figure 44 – Time-history record and plot for Unit 1D, December Test

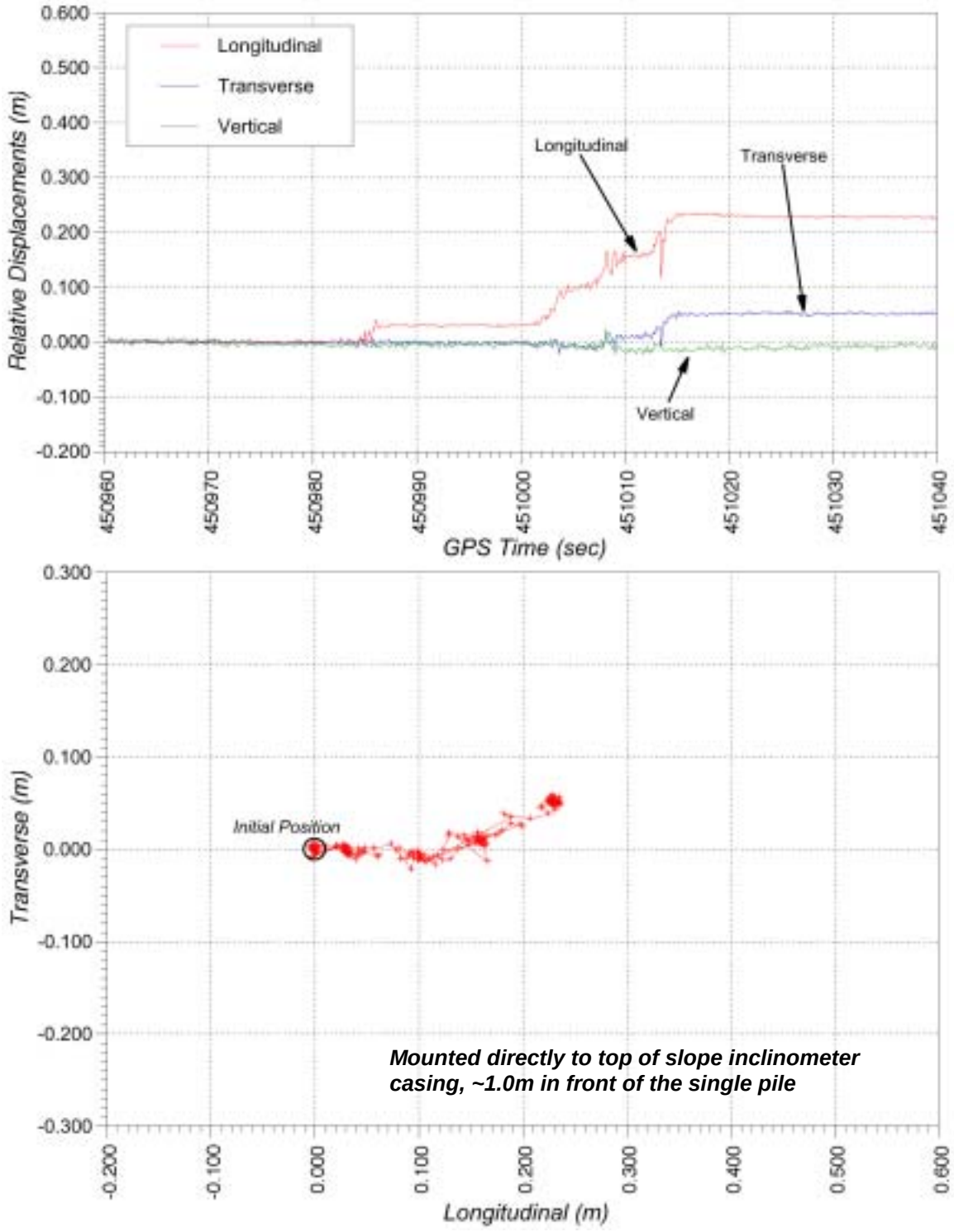

Figure 45 – Time-history record and plot for Unit 1E, December Test

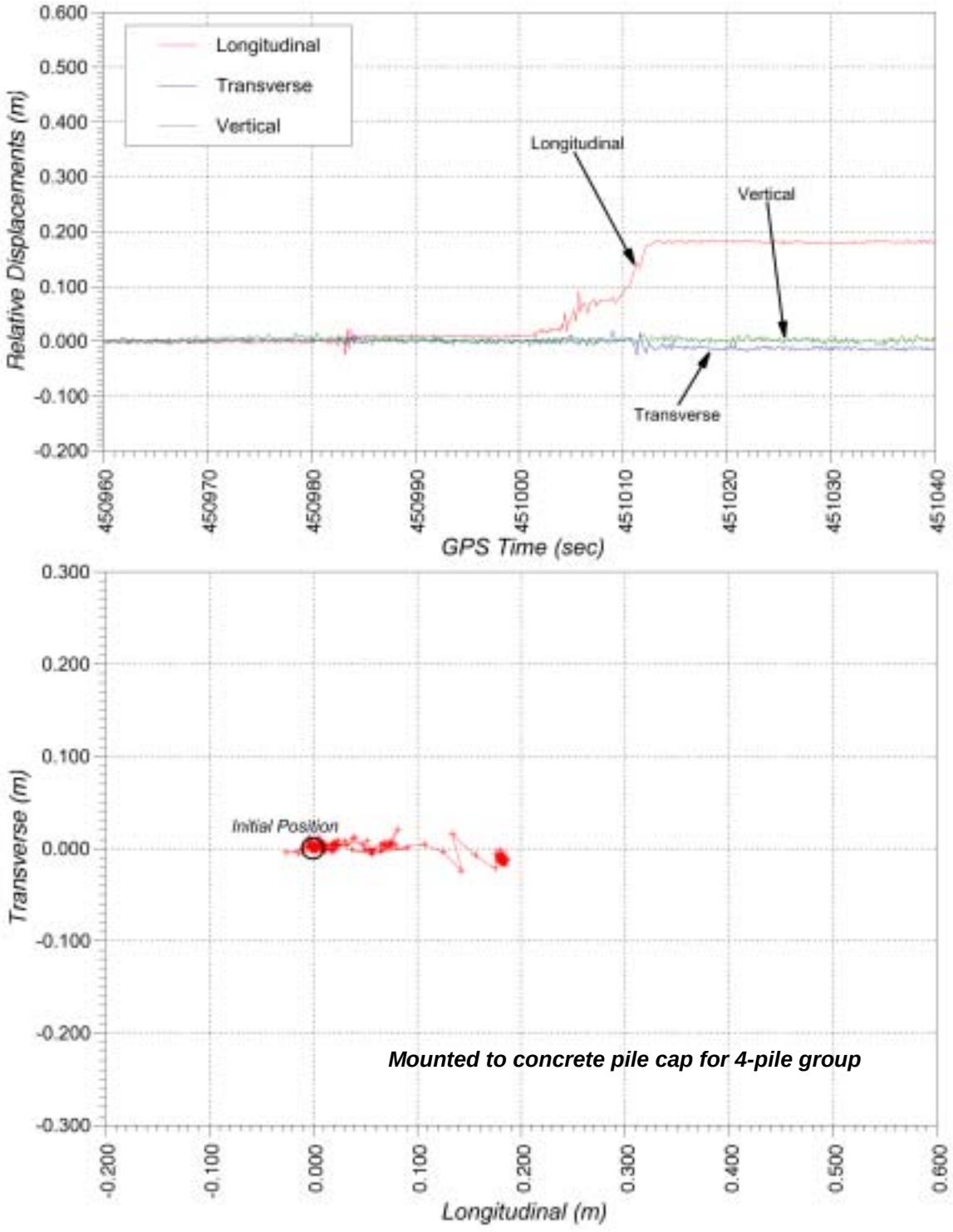

Figure 46 – Time-history record and plot for Unit 2A, December Test

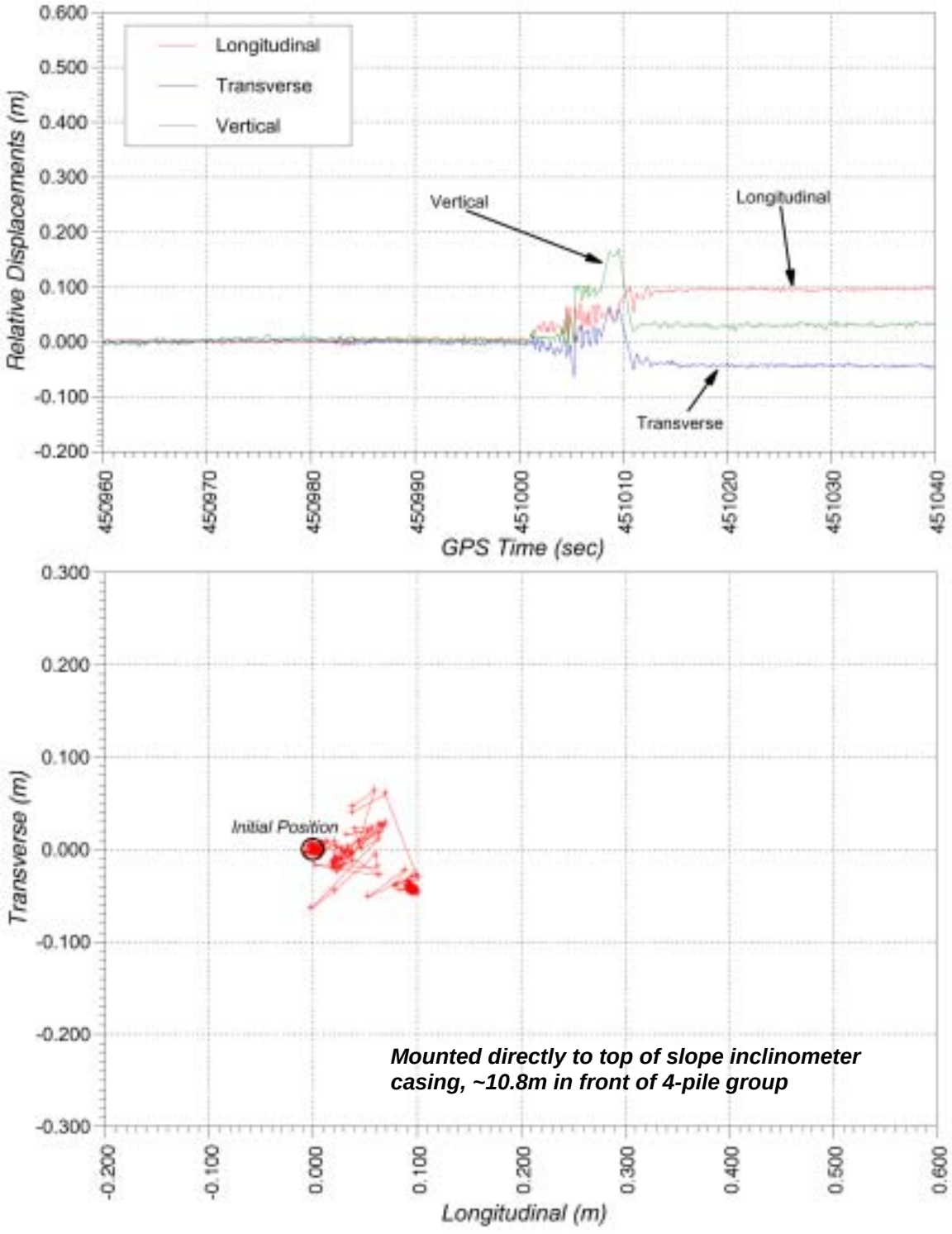

Figure 47 – Time-history record and plot for Unit 2B, December Test

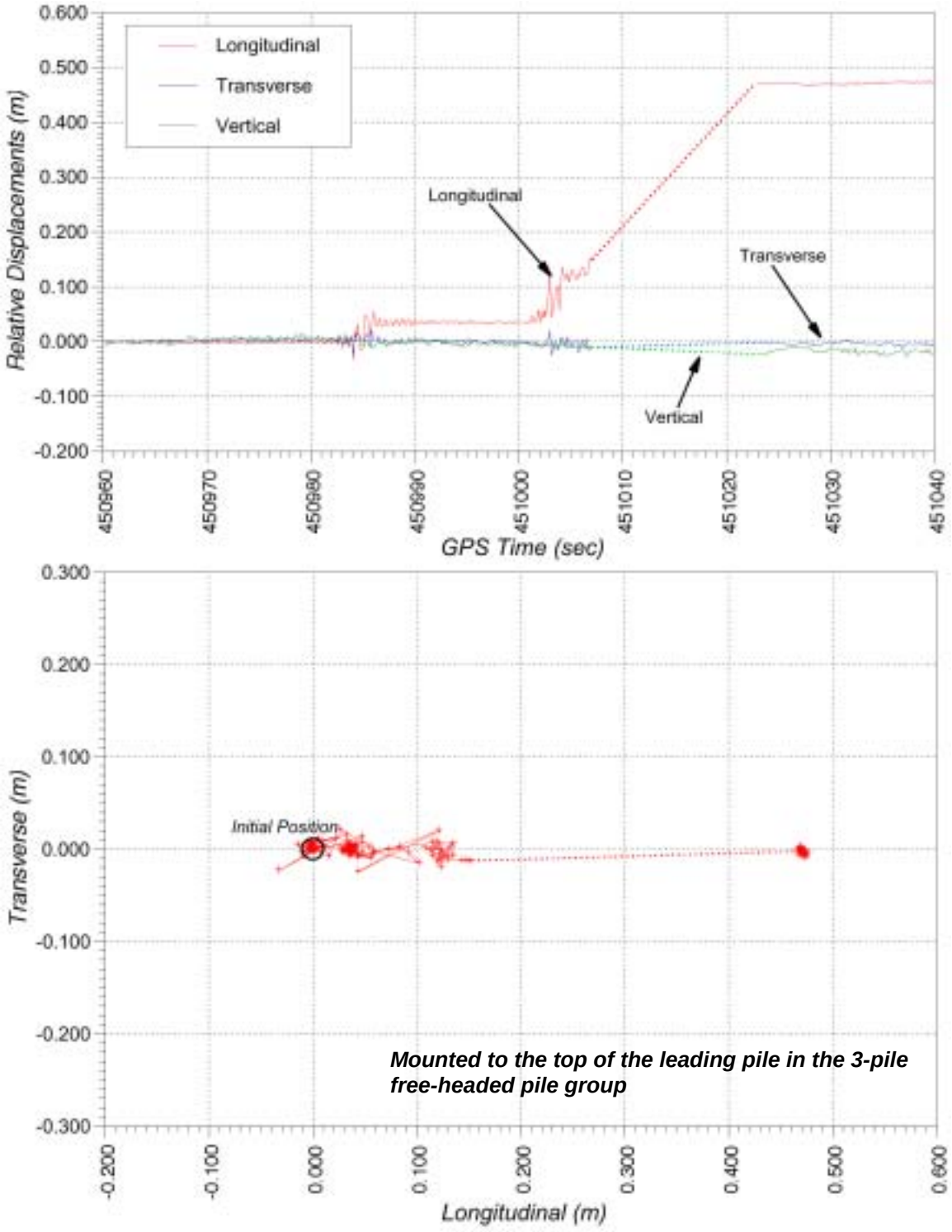

Figure 48 – Time-history record and plot for Unit 2C, December Test

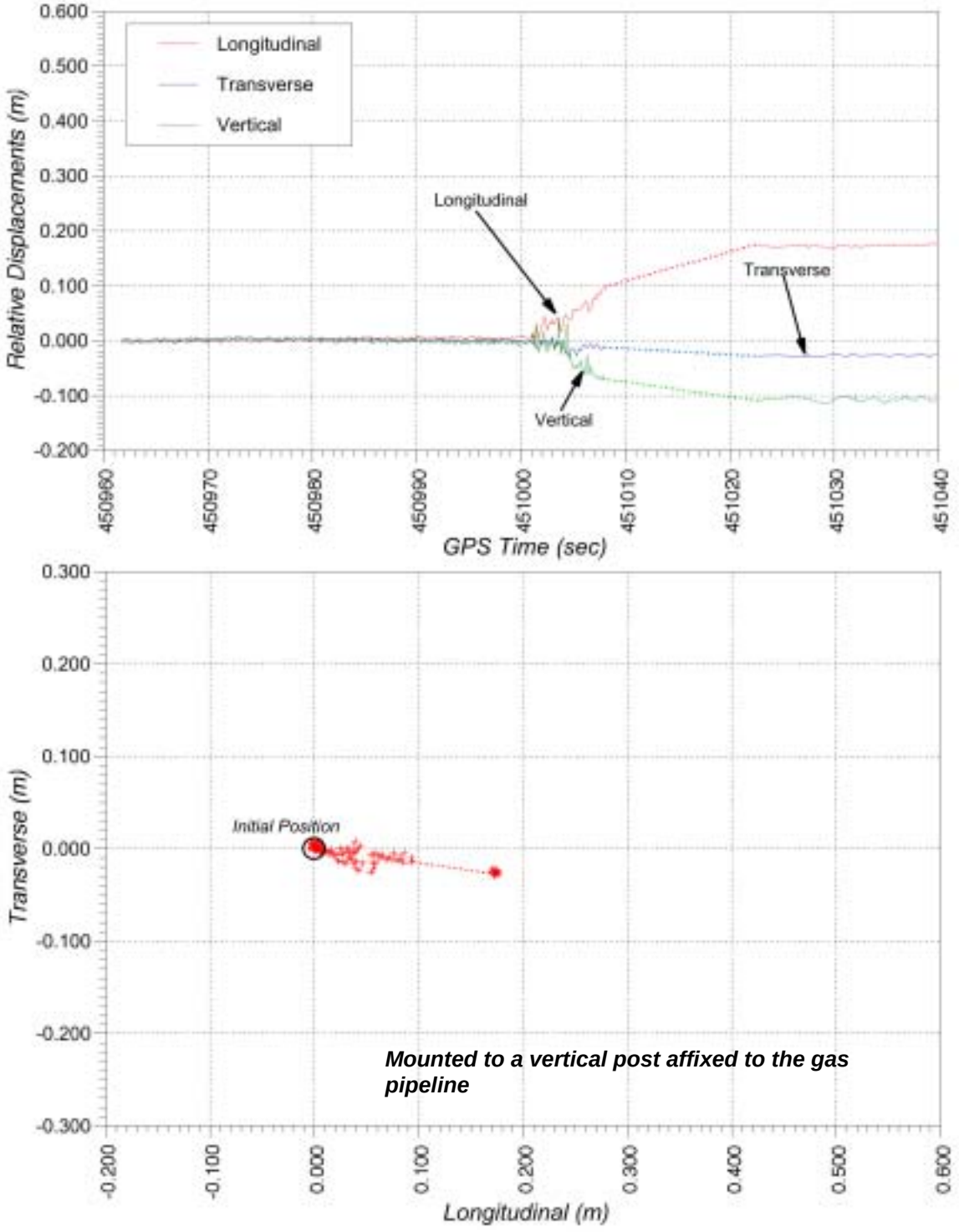

Figure 49 – Time-history record and plot for Unit 2D, December Test

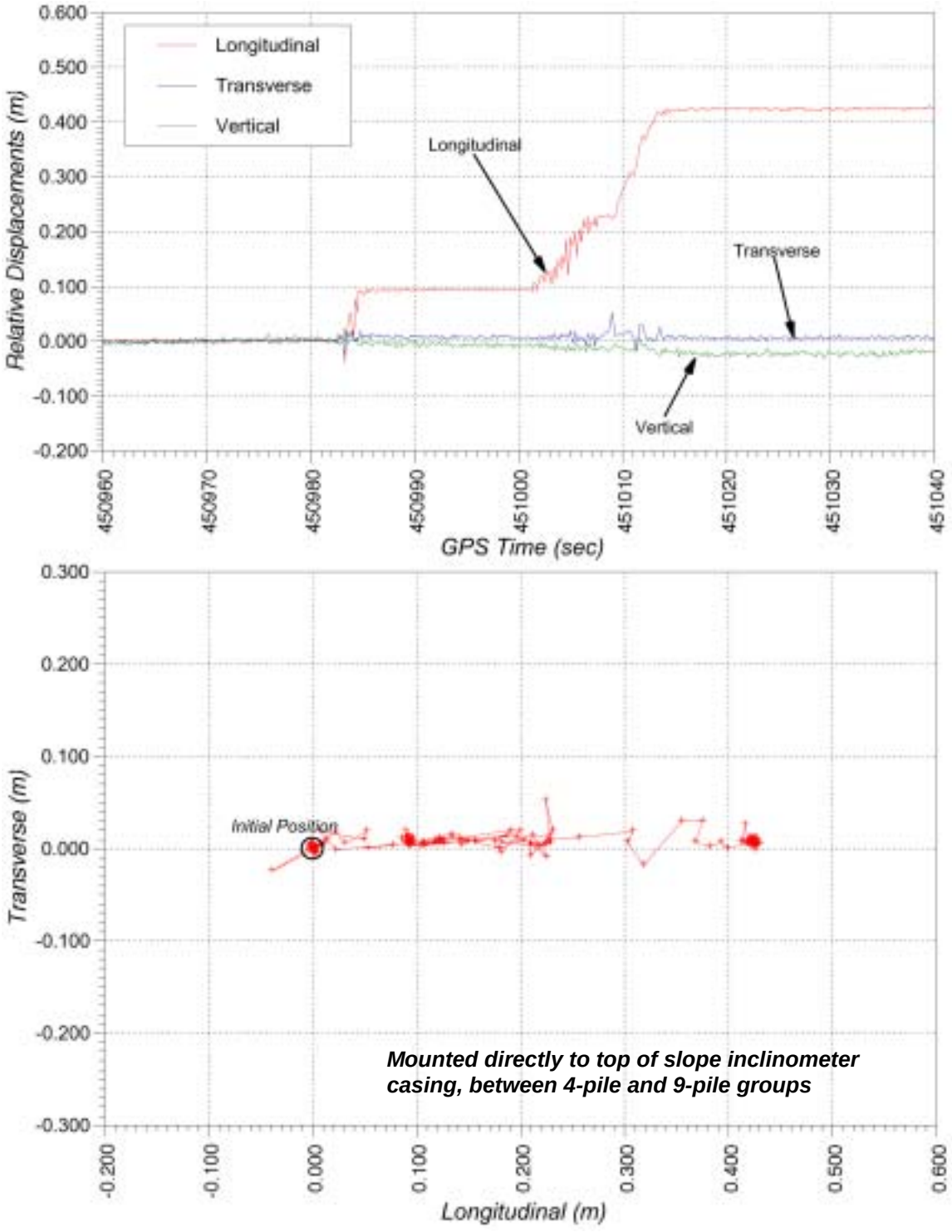

Figure 50 – Time-history record and plot for Unit 2E, December Test

3.2 General Discussion of Pre and Post-Blast Survey Results

Static measurements prior to and following the blasting provided important constraints on the short and long term displacement of the blast induced lateral spread. Dynamic measurements during the blast provided essential time history data to quantify the initiation, onset, and distribution of spread in time.

Positioning data for the tests were presented earlier in Tables 7 through 10 for measurements prior to, minutes after, and approximately 20 hours after the blasting. Significant displacements in the horizontal plane were measured and are summarized in vector displacement plots in Figures 52 and 53 for the November and December tests, respectively. These plots show the pre-blast antenna positions and the 20 hour post-blast positions (dashed line) of the GPS antennas. Horizontal displacement vectors are superposed on the plots and are shown with magnitudes multiplied by a factor of 10 for clarity.

The largest horizontal displacements measured during both tests were those for Unit 2C, mounted on top of the 3-pile group. Recall from Figure 16 that the GPS antenna was located approximately 1.8m above the ground surface. Following both tests, significant rotations were observed for all of the piles in the 3-pile group. Preliminary measurements from the November test showed that the pile to which Unit 2C was attached had rotated approximately 5º as shown in Figure 51. This rotation accounted for roughly 15cm of the 54.7cm total horizontal

displacement in the November test records. Similar pile rotations were observed in the December test. Tilt meter data collected by researchers from UCSD for both tests should be used and considered in future analyses when evaluating true ground deformations.

Figure 51 – Measuring rotation of pile, Unit 2C, November test

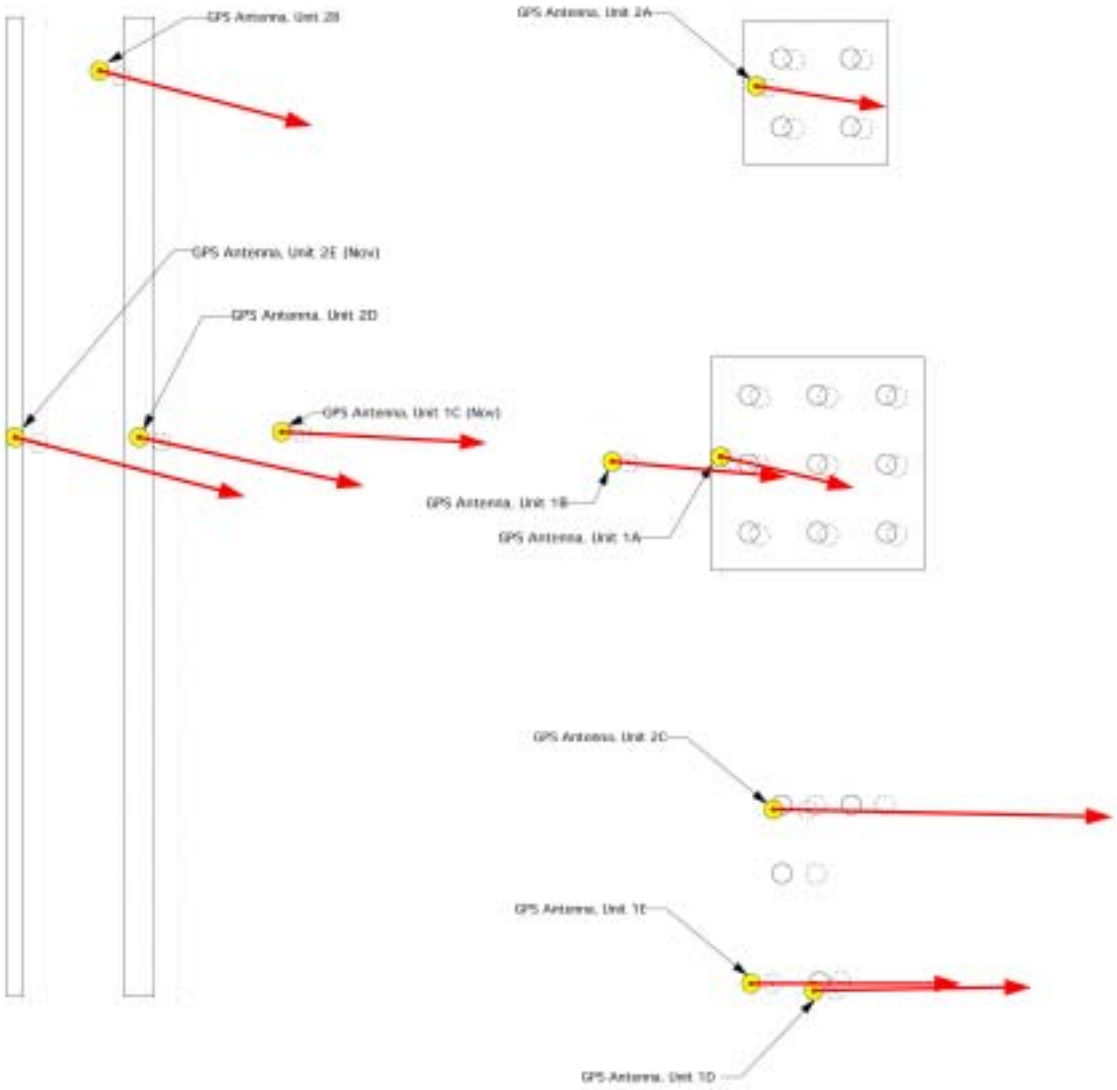

Figure 52 – Vector displacements in horizontal plane, November test

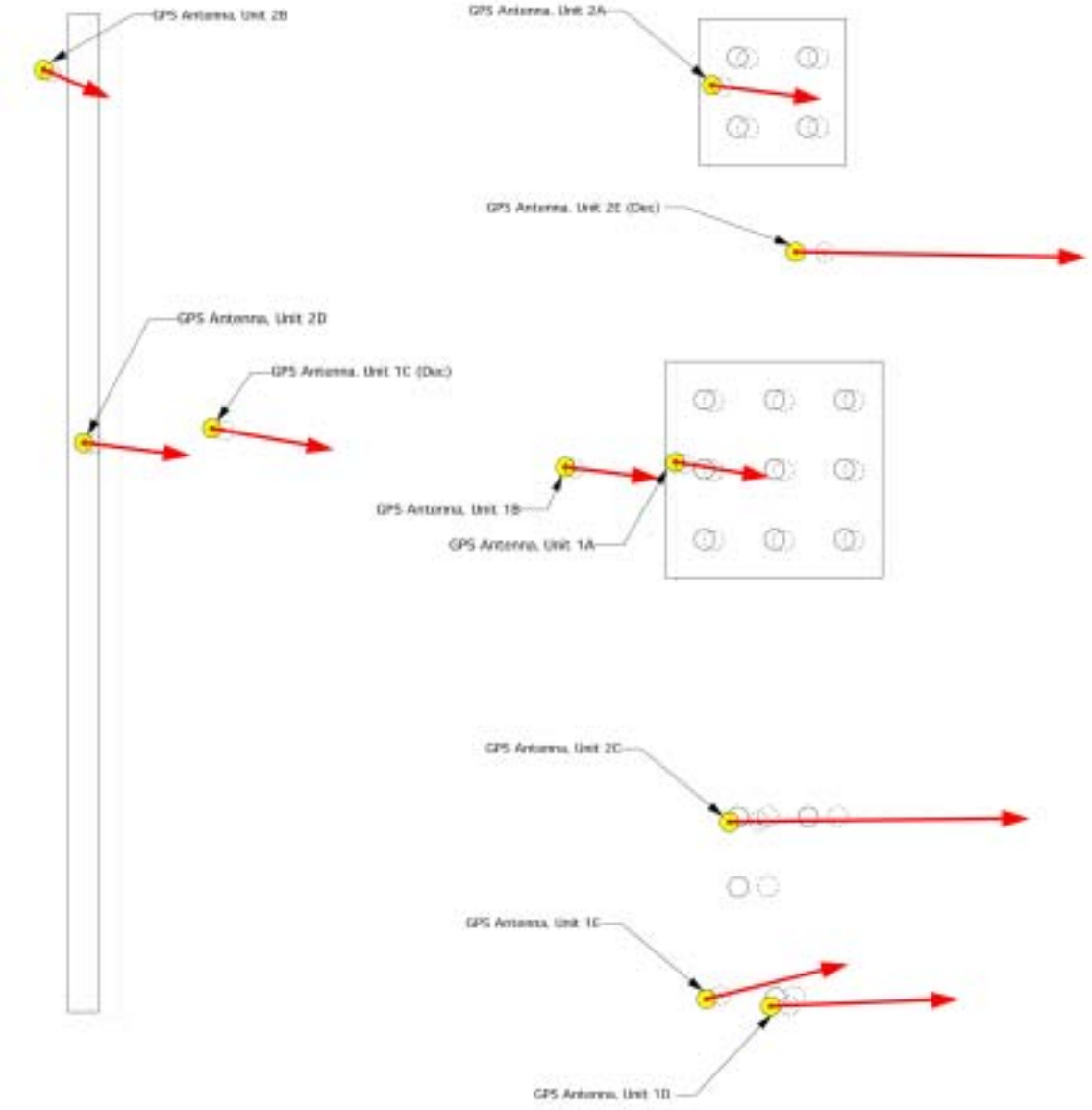

Figure 53 – Vector displacements in horizontal plane, December test

Significant deformations were observed in the vicinity of the pipelines during the November test. The two instrumented utility pipelines, Units 2D and 2E, as well as the free-field installation between the pipelines, Unit 2B, displaced approximately 35 to 38cm in the same direction with similar vertical settlements on the order of 9 to 13cm. These similar measurements could be interpreted in a number of ways. In one case, the pipelines may have constrained the movement of the upper soil layer during the lateral spread. Conversely, the pipelines may have deformed and displaced in unison with the surrounding soil during lateral spread. An examination of the strain results on the pipes from UCSD should provide clarity in the analyses.

Data on and near the 9-pile group provided measurements that substantiated the expected lateral spread behavior. Units 1B and 1C provided upstream near and free-field ground surface measurements for the 9-pile group. The large concrete pile cap and pile group was expected to restrict the flow of soil in that area. During the November test ground surface measurements decreased as they got closer to the pile cap with horizontal measurements of 33cm, 28cm, and 18cm, for Units 1C, 1B, and 1A, respectively. Similar behavior was observed during the December test with horizontal measurements of 20cm, 15cm, and 15cm, for Units 1C, 1B, and 1A, respectively. An additional measurement was taken during the December test next to the pile cap with Unit 2E. As much as 46cm of horizontal displacement was measured. This was significantly more displacement than that

measured at in the near and free-field units. However, it should be noted that as much as 10cm of the total 46cm can be attributed to a local slope failure near the waterway resulting from the preliminary blasting.

In general, larger displacements were recorded for the November test than in the December tests. Frozen surface soils are likely to have contributed to this.

The data presented in Tables 7 through 10 were examined to determine if any significant creep or settlement occurred between minutes and hours following the blasting. For both tests, it appears as though the horizontal ground displacements associated with the lateral spread took place over the limited period during, and within tens of seconds following blasting. In general, the changes in the measured horizontal positions over a 20 hour period were within the potential error margins for RTK-GPS.

Although horizontal creep was not observed over the 20 hours following blasting, the data revealed evidence of 9 to 13cm vertical settlement throughout the test site over an extended period of time as pore water pressures dissipated. Figure 54 shows the change in vertical position of the GPS antennas over time on a semi-log plot for both tests. The time prior to blasting is represented by t = 0.1sec. An initial data set collected following the blasting is shown at approximately 100 to 200sec. A final data set collected following the blasting is

shown at approximately 80,000sec. As much as 29cm of vertical heaving during the blasting was observed as was presented in Figures 35 through 50. However, this detail is not shown in the plots in Figure 54 to provide clarity to long-term trends.

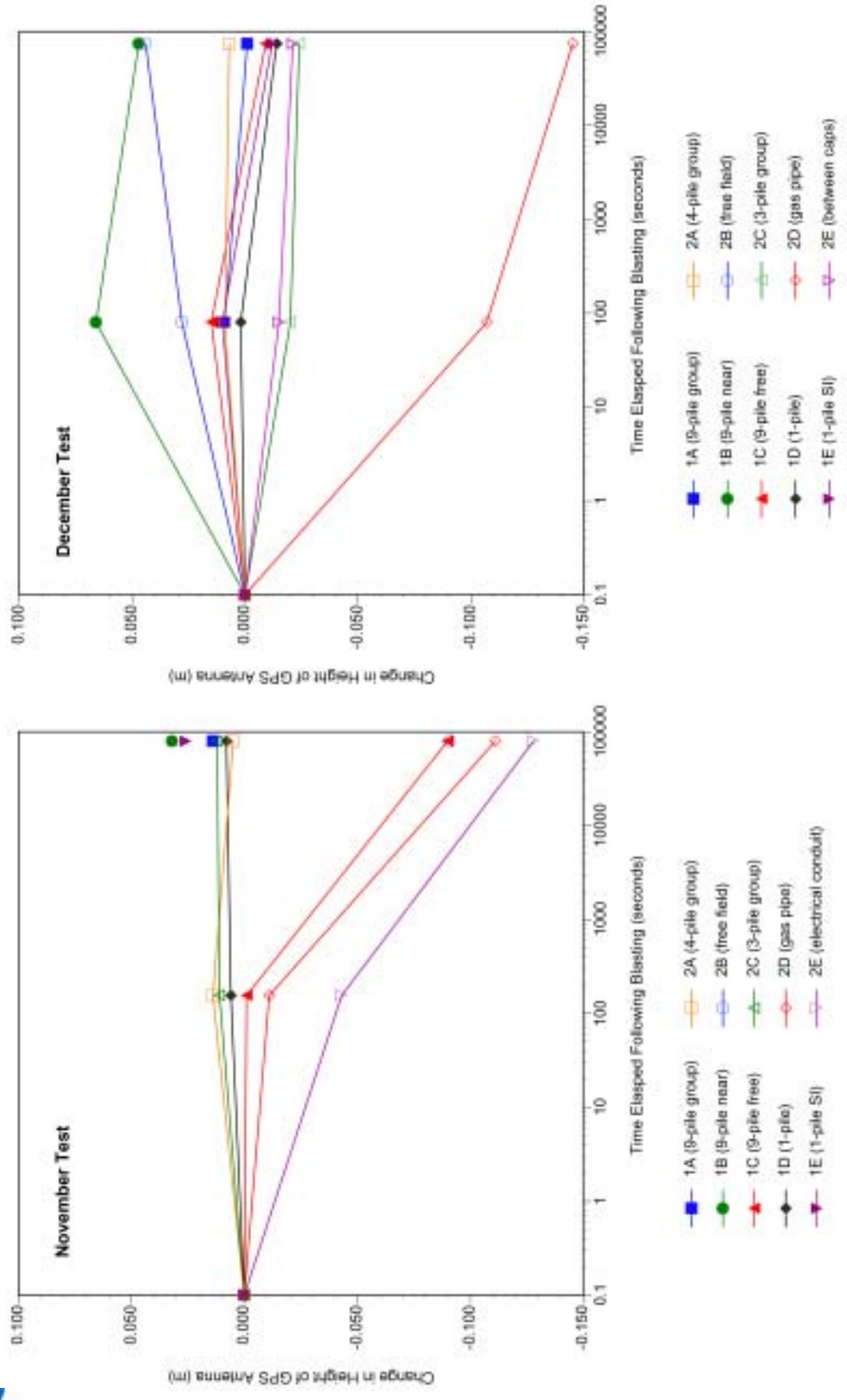

Figure 54 – Ground Surface Settlements, November Test (left), December Test (right)

During the November test significant settlements ranging from 9 to 13cm were measured for both free field installations (Units 1C and 2B) as well as for the two underground utilities (Units 2D and 2E). By contrast, measurements from the pile groups (Units 1A, 1D, 2A, and 2C) showed small upward heaving of less than 1cm during and following the blasting that did not subside over time. Although the vertical heaving estimates were near the vertical measurement resolution and could be attributed to measurement error, stability in the data trends seem to indicate otherwise. It is likely that short-term forces on the pipe piles from the blast induced soil heave displaced the piles upwards leaving a permanent vertical set. The GPS antennas installed directly onto slope inclinometer casings (Units 1B and 1E) showed evidence of permanent upward displacements between 2 to 3cm. Immediately following blasting, water was observed coming up through many of the inclinometer casings under high pressure. Figures 55 and 56 show photos of these observations after much of the water pressure was released. The release of pore water pressures through these casings in addition to potential buoyancy forces probably contributed to the upward movement of the casings. One of the inclinometer casings near the 4-pile group was observed to have risen in excess of 30cm as shown in Figure 57. Sand boils around the inclinometer casing can be seen in this photo.

Figure 55 – GPS Unit 1B shortly after blasting

Figure 56 – GPS Units 1D and 1E shortly after blasting

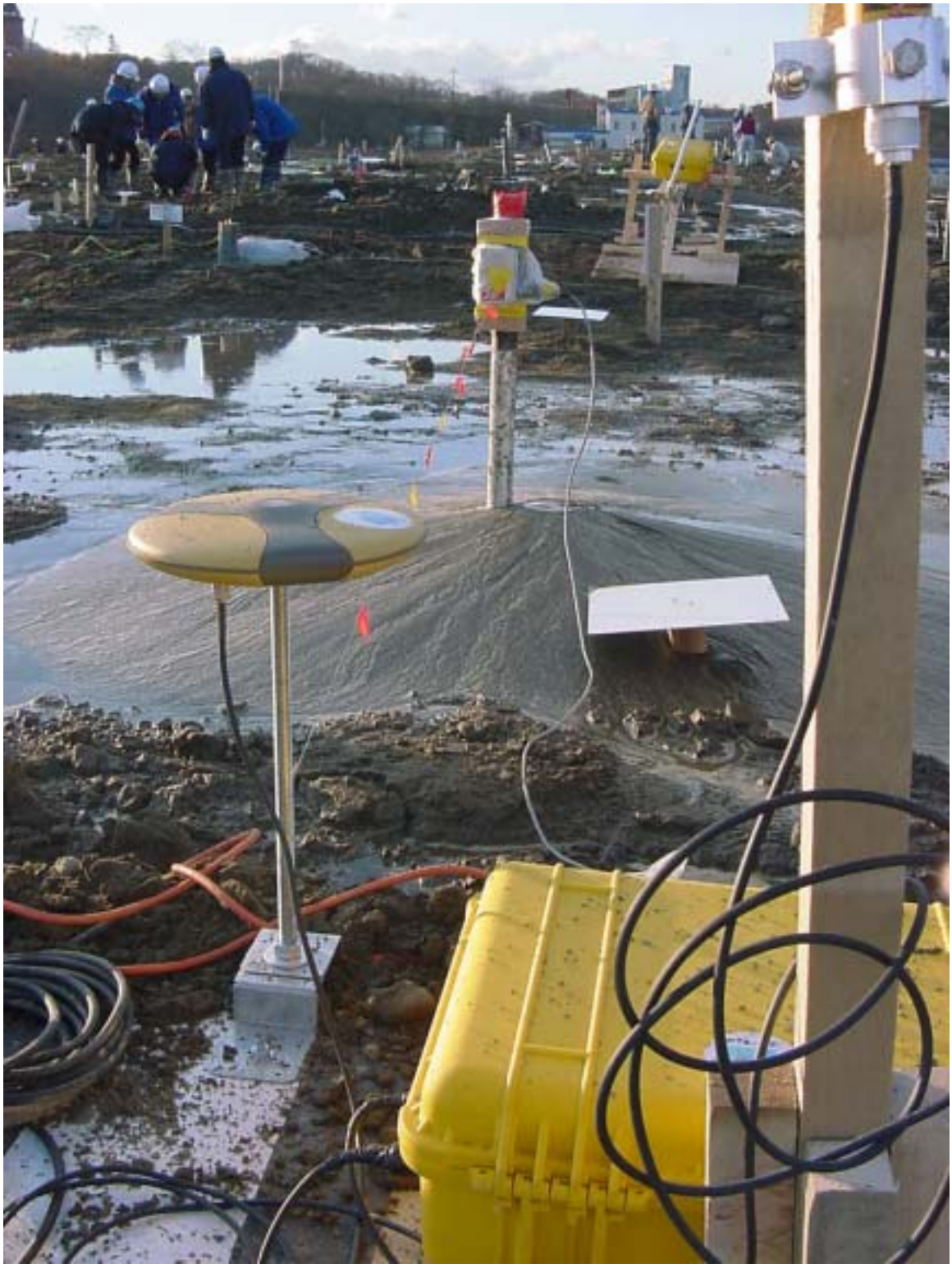

Figure 57 – GPS Unit 2A and adjacent inclinometer casing shortly after blasting

As was observed in the November test, the December test results showed significant settlement of the gas pipeline of approximately 14cm. However, unlike the November test significant settlements were not observed for the free field installations (Units 1C and 2B). In fact, Unit 2B showed an increase in vertical position of 4 to 5cm. As described elsewhere in this report, the GPS antennas for Units 1C and 2B were installed on rafts that were tied to adjacent slope inclinometer casings for the November test. This allowed the casing to rotate and move up and down without impacting the measurement of the location of the casing at ground surface. However, for the December test the GPS antennas were mounted directly to the inclinometer casings. Using this installation technique, the GPS could only capture the position of the top of the casing and not the true ground surface deformations. Snow buildup around the antenna mounts also made it difficult to assess relative changes between the casing and ground surface. Upward migration of pore water pressures through these casings in addition to potential buoyancy forces were likely to have caused many of the casings to rise such as measured with Units 1B and 2B.

3.3 General Discussion of Time-History Records

Detailed time-history records were presented in Figures 35 through 50 showing longitudinal, transverse, and vertical displacements over the period during blasting. These time-history records clearly illustrate the dynamic motion of the

ground surface or test specimen during blasting. Consider the time-history record for Unit 1C during the November test as shown in Figure 58 below.

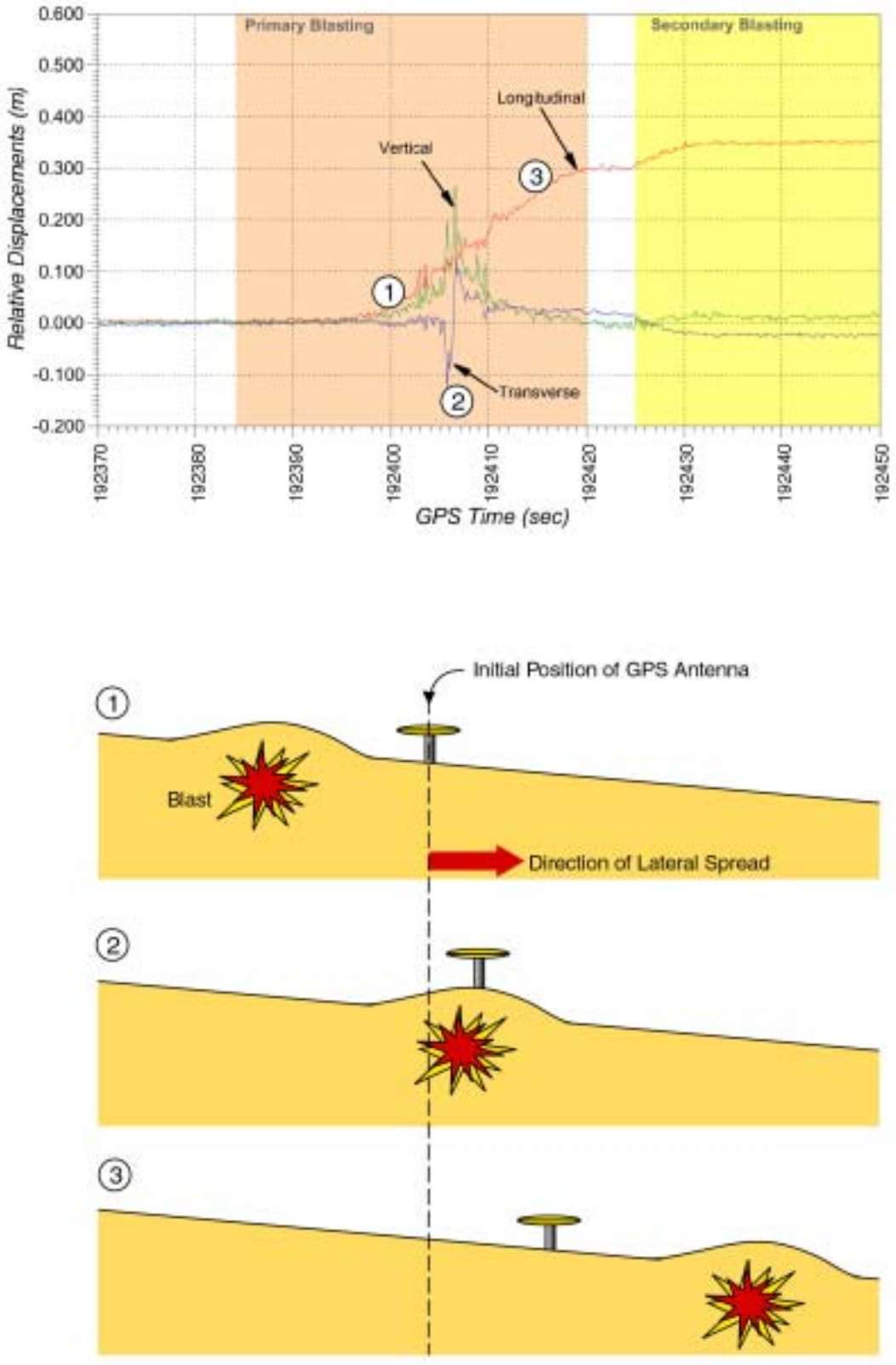

Figure 58 – Explanation of time-history record for Unit 1C, November test

As blasting proceeded from the back of the site to the front, compressive blasting forces raised pore water pressures throughout the site inducing liquefaction. The liquefaction, in turn, induced lateral spread, initiating longitudinal and vertical displacements as shown at time (1) in Figure 58. As blasting neared the location of the GPS antenna, greater deformations were recorded. Blasting near and below the location of the GPS antenna produced large vertical displacements and a quick transverse impulse as shown at time (2) in Figure 58. Recall from Figure 29 in Section 2.5 that the blasting proceeded sequentially in a series transverse rows. These transverse blasts were likely to have caused the large transverse motions in this particular record. Also notable, most of the GPS antennas were mounted on top of 5/8" threaded rod, cantilevered 15 to 30cm, which may have contributed to additional transient motions both transversely and longitudinally. With the blasting past the location of the GPS antenna, deformations were predominately longitudinal from lateral spread. Secondary blasting around the perimeter of the test site induced additional displacements.

As described earlier in the report, a short series of blasts to loosen the toe were executed prior to the primary blasting sequence for the December test. Most of the time-history records reflect the occurrence of this initial blasting. For example, in the record for Unit 2E the initial blast occurs at approximately 450983 sec as indicated as time (1) in Figure 59. This initial blast caused significant

longitudinal motions. The primary blasting began at approximately 451001 sec as noted by time (2), with completion of blasting at approximately 451013 sec as noted by time (3) in Figure 59.

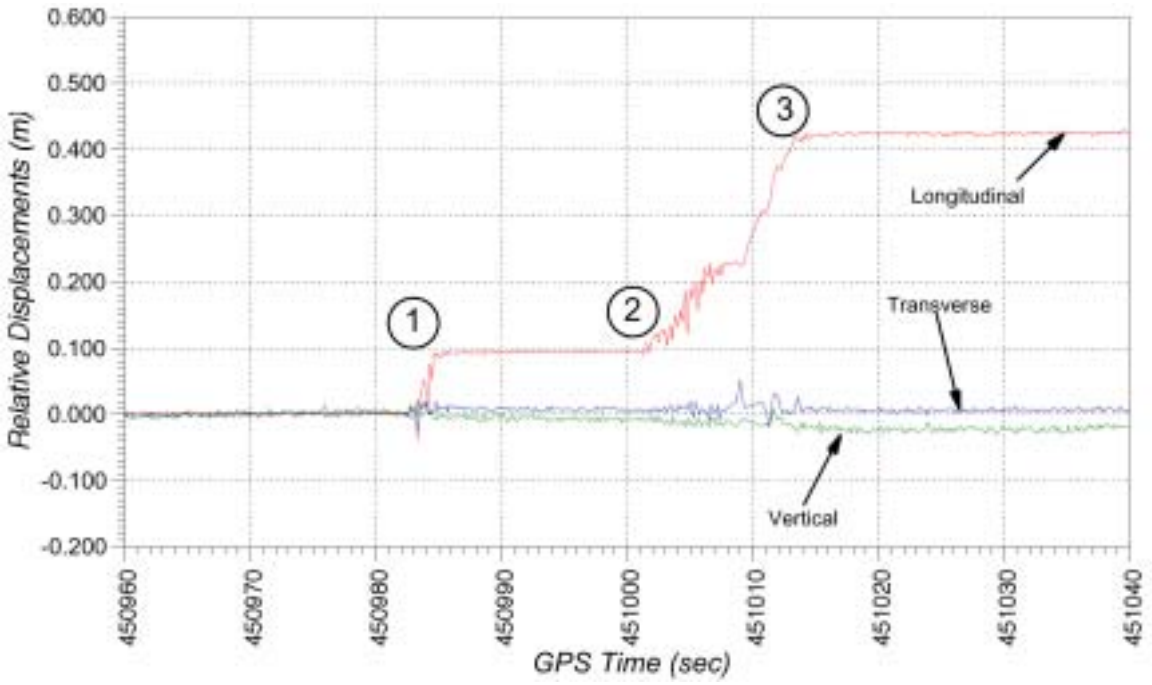

Figure 59 – Explanation of time-history record for Unit 2E, December test

3.4 Observations of Liquefaction from the November Test

During the November test, sensors attached to near the mid-span of the gas pipeline and electrical conduit provided a comprehensive data set on the initiation of liquefaction and ground surface deformations during blasting. Two GPS antennas, Units 2D and 2E, were installed at this location. Between the GPS antennas a research team from the UCSD had installed pore pressure transducers at multiple depths (Juirnarongrit 2002). Two of the three transducers in this area

provided pore pressure data, one installed at elevation –1.00m (designated as PPT-AB-4M) and the other at elevation –3.00m (designated as PPT-AB-6M). The groundwater elevation at the time of the test was approximately +0.50m. Figure 60 shows the 60 second time-history at this location as blasting passed through this area.

Multiple data sets are displayed in Figure 60. Data for GPS Units 2D and 2E are plotted using the scale on the right side of the plot, corresponding to the longitudinal component of displacement in the direction of the lateral spread. Data for pore pressure sensors PPT-AB-4M and PPT-AB-6M are plotted using the scale on the left side, expressed in terms of pore pressure ratio.

Recall that the pore pressure ratio, $\Delta\mu/\sigma_o'$, is the ratio of excess pore water pressure over the vertical effective overburden stress. Liquefaction has been defined by many as the stress state in which the excess pore water pressure, $\Delta\mu$, equals the effective stress, σ_o', in the soil (Kramer 1996). This can also be expressed as the condition where the pore pressure ratio, $\Delta\mu/\sigma_o'$, is equal to 1.

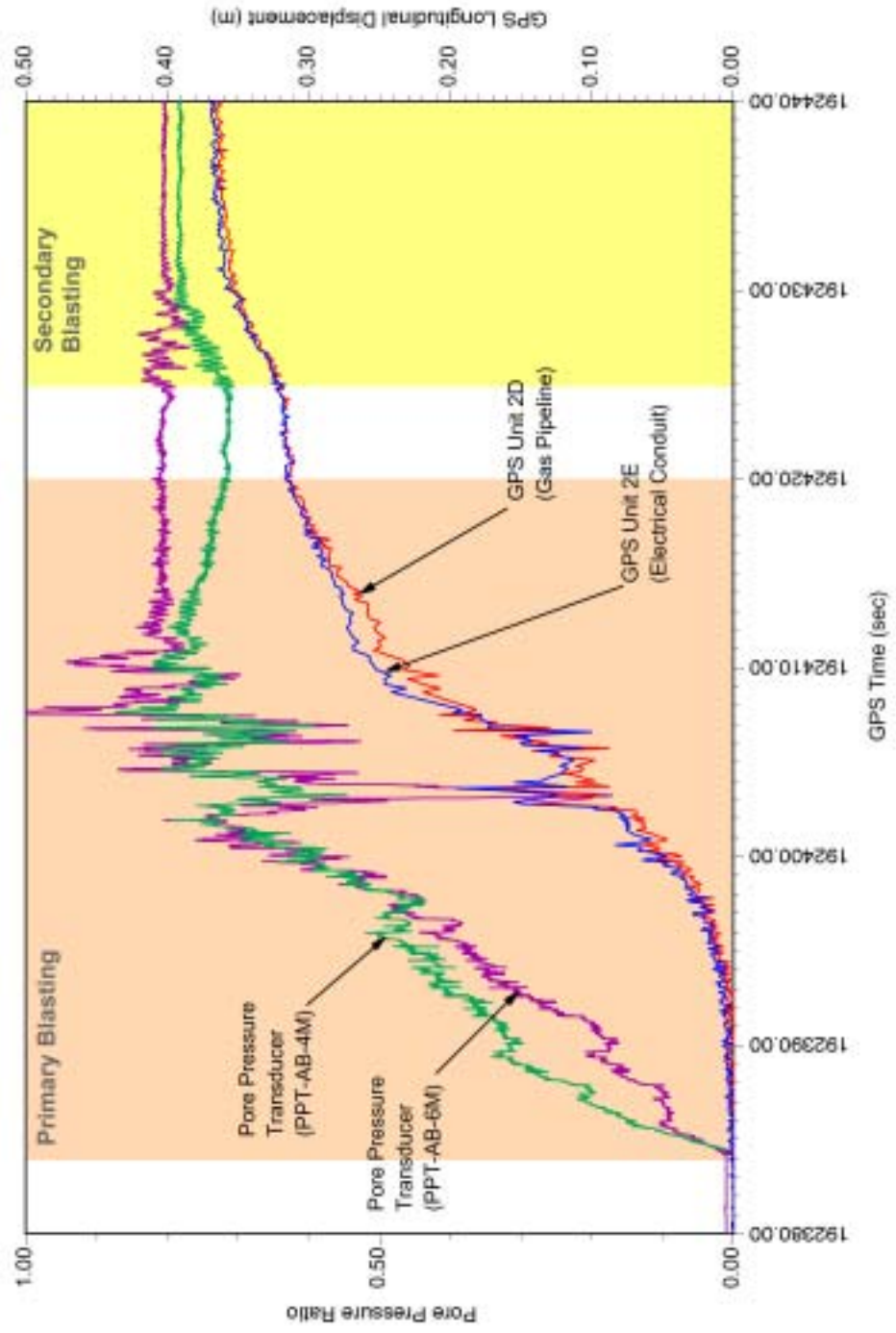

Figure 60 – Time-history of longitudinal displacement for GPS Units 2D and 2E, and filtered excess pore pressure for transducers PPT-AB-4M and PPT-AB-6M, November test

The GPS data shown in Figure 60 is displayed in an unfiltered 10Hz format. The raw pore pressure data was collected at 100Hz. However, to provide clarity in the plot, the raw pore pressure data was filtered using a 70 point (0.7 sec) centered moving average technique. The purpose of the filtering wasn't necessarily to reduce electrical noise, as is typically done in with transducer data in electrically sensitive environments. Compression waves from the sequential blasting leading up to and following the location of the pore pressure transducers created large spikes and drops in the data at a relatively high frequency. These spikes and drops appear similar to electrical noise, however are clearly discernable as p-waves or compression waves. Figure 61 shows an expanded time history of one of the pore pressure transducers during blasting.

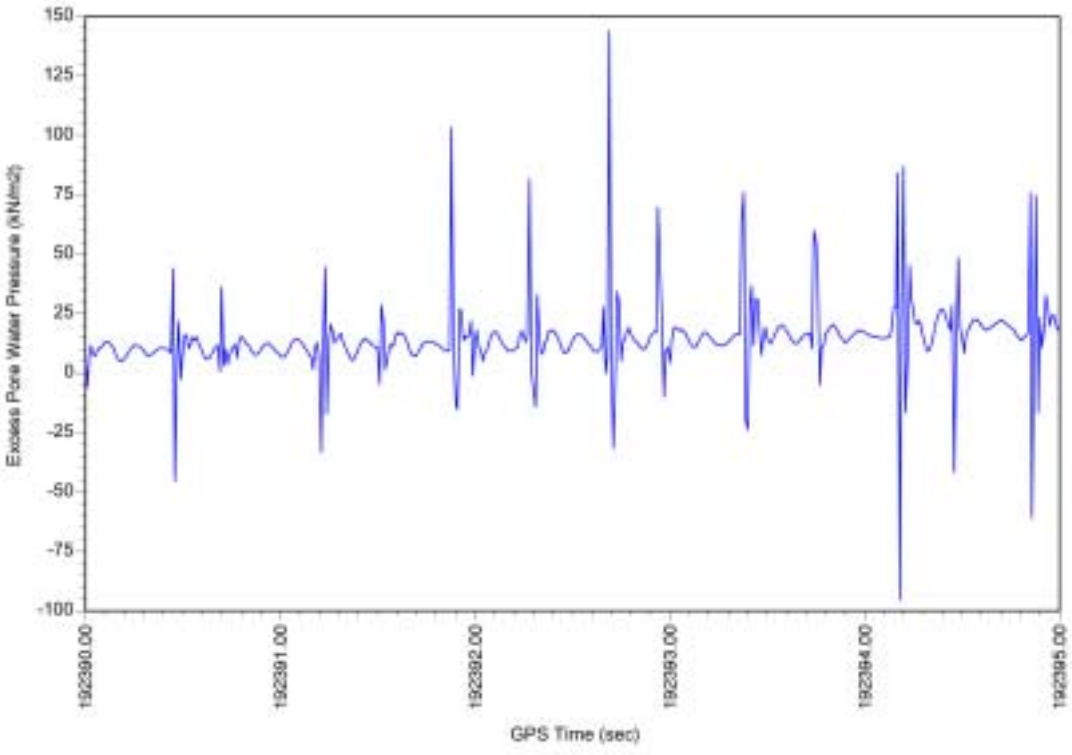

Figure 61 – Raw data time-history of excess pore pressure for transducer PPT-AB-4M

It is notable in Figure 61 that the data spikes occur at rate of about 2 per second. This rate is consistent with the timing of the primary blasting where 48 dual charges were detonated over a period of approximately 45 seconds.

Examining the plot in Figure 60, longitudinal ground surface deformations are first detectable between approximately 192384.2 and 192384.3 seconds, GPS time, with the pore pressure transducers showing a rapid increase during that same time interval. Since the blasting commenced at 192384.30 seconds, it is clear from the data that significant increases in both pore pressures and displacements occurred simultaneously at the onset of blasting and with pore pressure ratio at only 0.1.

The first blast in the primary sequence of blasting was detonated approximately 40 meters away from the location of the pore pressure transducers as was shown in Figure 29. As blasting progressed through the site, pore pressures increased relatively linearly in time from 192384.30 seconds to approximately 192403.00 seconds, the estimated time of the blast in the hole closest to the pore pressure transducers. Pore pressure measurements were somewhat erratic between 192403.00 seconds and 192413.00 seconds resulting from the nearby blasting, but leveled off with mean values ranging between 0.75 and 0.80.

Small but steady longitudinal displacements were measured from the onset of blasting at 192384.30 seconds up to approximately 192398.00 seconds, after which time the rate of motion increased significantly with pore pressure ratios in excess of 0.5. The rate of longitudinal displacements decreased after 192410.00 seconds. Pore pressure measurements from PPT-AB-4M indicated some dissipation at this time as well. Secondary blasting around the perimeter of the test site, beginning at approximately 192425 seconds, created additional deformations and a modest increase in pore pressure ratio for PPT-AB-4M back to its previous levels.

Based upon the measurements it appears that the ground movements were likely generated by a combination of blasting forces as well as lateral spread from liquefied soils. The smaller displacements at the onset of blasting (192384.30 to 192398.00 seconds) were likely due to a combination of compressive downslope forces created by spreading soil upslope and weakened soil near the GPS unit resulting from increased pore pressures. Although pore water pressure ratios were relatively low during this time period, ranging from 0 to 0.50, this may have been sufficient to induce some weakening of the soil. As blasting passed through this location, pore pressures reached peak ratios, the soil was nearing a liquefied state, and lateral spread was observed with an increased rate of displacement (192398.00 to 192410.00 seconds). As blasting proceeded in front of the location of the GPS units, compressive blast forces acting in the opposing

direction may have contributed to the decrease in the rate of longitudinal displacement (beyond 192410.00 seconds). Since the GPS units were attached directly to the utility pipelines, the decrease in the rate of longitudinal displacement may have also been due to resistance from the flexure in the pipelines. Free-field measurements between the pipelines from Unit 2B showed displacements of similar magnitude and direction as those of the pipelines. However, since the Unit 2B was installed in the area of engineered backfill around the pipelines, it may not be a reliable indicator of true free field ground motions. Subsequent analysis of stresses in the pipelines may resolve this question.

3.5 Validity of Measurements

At a couple of locations, measurements with GPS were checked against secondary extensometer measurements. The UCSD research team installed one extensometer between GPS Units 1A and 1B which spanned the distance between the 9-pile group cap and the near-field slope inclinometer casing (Juirnarongrit 2002). Another extensometer was installed between GPS Units 1D and 1E which spanned the distance between the single free-head pile and the near-field slope inclinometer casing adjacent to it. A summary of the relative displacements is shown in Table 11 based upon data collected during the November test. These measurements represent the change in total distance,

vector sum of horizontal and vertical, between the two sets of GPS antennas as determined independently from GPS and extensometer measurements.

Location	GPS Measurement	Extensometer Measurement
GPS Units 1A and 1B	0.105m	0.096m
GPS Units 1D and 1E	.009m	.006m

Table 11 – Validation of GPS Measurements

In general, the extensometer data confirmed the GPS measurements. At both locations the GPS measurements were within 1cm of the extensometer measurements, which is the accuracy typically associated with RTK-GPS methods.

4.0 Conclusions

This report presented deformation measurements developed using RTK-GPS for two full-scale lateral spread tests in Japan in November and December 2001. Subsequent analysis of the data sets will be used by others to model the test events to gain new insight into the performance of pile foundation systems and pipelines during earthquakes.

The test deployment in Japan demonstrated the flexibility and stability of the integrated GPS based deformation monitoring system at its current stage in development under severe inclimate weather and turbulent environments. GPS

measurements provided an otherwise unattainable data set for this type and scale of test.

5.0 Acknowledgements

The assistance of Professor Scott Ashford from the University of California San Diego (UCSD) in leading the overall U.S. effort in designing the lifeline experiment and coordinating with the Japanese colleagues is gratefully acknowledged. Cliff Roblee and Tom Shantz from Caltrans' Division of New Technology and Research are also acknowledged for their help in setting up the GPS equipment. The author would also like to recognize the outstanding coordination provided by Dr. Sugano of PARI in effectively managing the site and the many contractors and research teams. Finally, the assistance of Cliff Roblee and Tom Shantz in providing comments on the early draft of this report is greatly appreciated.

6.0 References

Ashford, S.A., Elgamal, A., and Uang, C. (2001). *Performance of Lifelines Subjected to Lateral Spreading: Full-Scale Experiment,* Department of Structural Engineering, University of California, San Diego. (Project Proposal).

Dana, P.H., (1994). *"Global Positioning System Overview," The Geographer's Craft Project, Department of Geography, The University of Colorado at Boulder,* <http://www.colorado.Edu/geography/gcraft/notes/gps/gps_f.html> (April 11, 2003).

Hofmann-Wellenhof, B., Lichtenegger, H., and Collins, J. (1997). *GPS Theory and Practice,* Springer-Verlag, Wien, New York.

Holtz, R.D. and Kovacs, W.D. (1981). *An Introduction to Geotechnical Engineering,* Prentice-Hall, Inc., Englewood Cliffs, New Jersey.

Juirnarongrit, T. (2002). *(Personal Communication between January 1 to March 13, 2002),* Department of Structural Engineering, University of California San Diego.

Kramer, S.L. (1996). *Geotechnical Earthquake Engineering,* Prentice Hall, Inc., Upper Saddle River, New Jersey.

Langley, R.B. (1998). *"RTK GPS," GPS World Magazine*, September 1998.

Turner, L., (2000). *Stage 1 Report, Continuous GPS: Pilot Applications*; Caltrans Internal Report to the Project Advisory Panel.

Turner, L., (2001). *Stage 2 Project Status Report, Continuous GPS: Pilot Applications*; Caltrans Internal Report to the Project Advisory Panel.

Waypoint Consulting, Inc.. (2000). *RTKNav, Rt Engine Rt DLL Windows 95/98/NT Real-time GPS Processing Software*, (Software Manual), Calgary, Alberta, Canada.